




Optimal antimicrobial dosing combinations when drug-resistance mutation rates differ

Oscar Delaney^{1*}  Andrew D. Letten¹  Jan Engelstädter¹ 

¹School of the Environment, The University of Queensland

* correspondence addressed to o.delaney@uq.net.au

March 18, 2025

Abstract

Given the ongoing antimicrobial resistance crisis, it is imperative to develop dosing regimens optimised to avoid the evolution of resistance. The rate at which bacteria acquire resistance-conferring mutations to different antimicrobial drugs spans multiple orders of magnitude. By using a mathematical model and computer simulations, we show that knowledge of relative mutation rates can meaningfully inform the optimal combination of two drugs in a treatment regimen. We demonstrate that under plausible assumptions there is a linear relationship in log-log space between the drug A :drug B dose ratio that maximises the chance of treatment success and the ratio of their mutation rates. This power law relationship holds for bacteriostatic and bactericidal drugs. If borne out empirically, these findings suggest there might be significant room to further optimise antimicrobial dosing strategies.

Keywords: microbial evolution, mutation rates, mathematical modelling, antimicrobial resistance, combination therapy, evolutionary rescue.

1 Introduction

One of the key goals of designing antimicrobial treatment regimens must be to minimise the probability that resistance develops, alongside striving to rapidly clear the patient's infection and avoid excessive toxicity. One valuable approach is to use multiple drugs, either in combination [1, 2] or sequentially [3, 4, 5, 6] such that even if a mutation conferring resistance to a single drug occurs, the mutant is still impacted by the other drug(s). Using multiple drugs, rather than just a larger dose of a single drug, may also reduce toxic side effects in the patient, especially if the drugs interact synergistically and hence allow for smaller concentrations to be

28 efficacious [7]. Combination therapy is supported by a significant body of empirical literature
29 (reviewed in [8] and [9]), with positive results for example in laboratory evolution settings [1]
30 and tuberculosis treatment [10]. A meta-analysis involving 4514 patients from 53 studies of
31 multidrug-resistant gram-negative bacterial infections found an average reduction in mortality
32 of 17% with combination compared to monotherapy [11].

33 Many mathematical and computational models have been created to better understand and
34 predict the evolution of resistance (reviewed in [12, 13]). In most models, a key parameter
35 is the mutation rate: the probability that a cell division in a susceptible bacterium will give
36 rise to a cell resistant to the drug in question. The higher the mutation rate, the more likely
37 resistance is to develop (setting aside resistance arising from horizontal gene transfer). Because
38 this relationship is trivial, in most mathematical models the mutation rate is fixed and then
39 ignored, and other putatively more interesting phenomena are explored [14, 15, 16, 17, 18].
40 Here, we show that in combination therapy, the relative mutation rates for each drug can be an
41 important factor in choosing the optimal quantity of each drug to apply. This differs notably
42 from the conventional wisdom that it is often best to use equal doses of two drugs (e.g. [19]).

43 An important consideration in combination therapy is whether to use bacteriostatic drugs
44 (i.e. drugs that inhibit growth), bacteriocidal drugs (i.e. drugs that kill bacteria), or both.
45 Theoretical work has shown that when only one drug is present at a time, bacteriostatic drugs
46 are usually more effective in minimising resistance evolution [20]. When two drugs are used in
47 combination, theory suggests that pairing a bacteriostatic drug and a bacteriocidal drug is espe-
48 cially effective at both clearing the infection and reducing the probability of resistance evolving
49 [19]. Moreover, the density-dependence and resource limitations of the bacterial population
50 impact the relative efficacy of different drug modes of action [21].

51 The rate at which resistance mutations to a given antimicrobial drug occur may depend
52 on the bacterium that is targeted, the current resource availability or other environmental
53 conditions. Even within one host species and constant conditions, resistance mutation rates
54 can vary greatly by drug [22]. This is unsurprising, as different mechanisms of action may
55 be more or less difficult for the bacteria to surmount or circumvent when sampling from the
56 space of possible mutations. The distribution of fitness effects of possible resistance mutants
57 can also vary greatly by type of drug used [23]. In *Mycobacterium tuberculosis*, the infectious
58 agent responsible for the most deaths per year worldwide [24], there is an approximately 400-
59 fold difference in the mutation rate between two of the most commonly used first-line drugs,
60 rifampicin and ethambutol [25]. That said, it is difficult to accurately compare estimated
61 mutation rates for different drugs. This is because the mutation rate may depend on the
62 drug concentration used (the higher the concentration, the fewer resistance mutations may be
63 possible), and also because the stress response to some drugs may elevate the mutation rate
64 itself [26]. To our knowledge, there is no centralised database of mutation rate estimates, but
65 some example values from the literature for various drugs and species are provided in Table
66 1. Resistance mutation rates being orders of magnitude apart could reasonably be expected
67 to prove important when choosing optimal dosing strategies. Intuitively, all else being equal,

68 it is better to use drugs for which resistance mutations arise at a lower rate to minimise the
69 probability of resistance developing.

70 We formalise and interrogate this intuition under a variety of plausible assumptions, and
71 develop theoretical predictions for how different resistance mutation rates should alter optimal
72 dosing strategies. We find that a quadrupling of the ratio of mutation rates leads to a doubling
73 in the optimal drug dosing concentration ratios favouring the less evolvable drug. This power
74 law relationship is qualitatively robust to relaxing various simplifying assumptions.

Table 1: Genome-wide probability of a resistance mutation per replication for various antibiotics in *Mycobacterium tuberculosis*, *Mycobacterium smegmatis*, and *Escherichia coli*.

Drug ($\mu\text{g/mL}$)	Bacteria	Mutation probability (μ)	References
Isoniazid (0.2 to 1)	<i>M. tuberculosis</i>	$2.6 \cdot 10^{-8}$ to $3.2 \cdot 10^{-7}$	[25, 27]
Rifampicin (1 to 8)	<i>M. tuberculosis</i>	$2.3 \cdot 10^{-10}$ to $1.1 \cdot 10^{-8}$	[25, 27, 28]
Streptomycin (2)	<i>M. tuberculosis</i>	$3.0 \cdot 10^{-8}$	[25]
Ethambutol (5)	<i>M. tuberculosis</i>	$1.0 \cdot 10^{-7}$	[25]
Rifampicin (100 to 500)	<i>M. smegmatis</i>	$2.2 \cdot 10^{-10}$ to $9.2 \cdot 10^{-8}$	[29]
Isoniazid (500 to 1000)	<i>M. smegmatis</i>	$1.2 \cdot 10^{-9}$ to $1.2 \cdot 10^{-7}$	[29]
Streptomycin (20 to 100)	<i>M. smegmatis</i>	$2.8 \cdot 10^{-8}$ to $5.3 \cdot 10^{-8}$	[29]
Kanamycin (100)	<i>M. smegmatis</i>	$1.7 \cdot 10^{-8}$	[29]
Rifampicin (50)	<i>E. coli</i>	$7.0 \cdot 10^{-9}$	[30]
Streptomycin (2)	<i>E. coli</i>	$2.7 \cdot 10^{-9}$	[31]
Ciprofloxacin (1)	<i>E. coli</i>	$3.6 \cdot 10^{-9}$	[32]

75 2 Methods

76 We modelled a simple scenario where there is one species of bacteria and two arbitrary drugs,
77 A and B , administered in combination at concentrations C_A and C_B that are constant over
78 time (we later relax this assumption). After t hours the sizes of the susceptible, A -resistant,
79 and B -resistant populations respectively are $S(t)$, $M_A(t)$ and $M_B(t)$.

80 To model drug mode of action and pharmacodynamics, we normalised the effective drug
81 concentration (E_i) for bacterial strain $i \in \{S, M_A, M_B\}$ (that is, susceptible, A -resistant mu-
82 tants, and B -resistant mutants respectively) and drug $j \in \{A, B\}$ onto the $[0, 1)$ interval using
83 the sigmoid E_{\max} model [33] (closely related to the more common Hill equation [34]). Here,
84 $z_{i,j}$ is the drug concentration at which the half-maximal effect of drug j is achieved in strain
85 i (denoted EC_{50} in [35]) and β is the shape parameter which determines the steepness of the
86 function around z [36]:

$$E_i(C_j) = \left(1 + \left(\frac{C_j}{z_{i,j}} \right)^{-\beta_j} \right)^{-1}. \quad (1)$$

87 Here, complete resistance ($E_i(C_j) = 0$ for any C_j) would arise with $z_{M_A,A}, z_{M_B,B} \rightarrow \infty$.
88 We consider drugs that are either bacteriostatic (denoted $\phi_j = 1$) and only affect the cell

89 division rate, or bactericidal (denoted $\phi_j = 0$) and only affect the cell death rate, leaving out
 90 intermediate cases. We ignored the effect of intra-specific competition on growth, such that
 91 the replication rate of strain i is a constant r_i in the absence of drugs (this assumption is
 92 later relaxed in the simulations, but is necessary for analytical progress). While in most cases
 93 bacterial growth is resource-limited such that our analytical model would be unrealistic, in some
 94 cases e.g. if antibiotic treatment is started early by the human host before pathogenic bacteria
 95 have reached the resource limits of their niche, our model could be [more realistic](#)
 96 [accurate](#). Likewise, δ_i is a constant intrinsic death rate term, representing constant negative
 97 pressures from competition with other (non-modelled) bacterial species [37], and the host's
 98 immune response. Combining, the drug-dependent replication, death, and net growth rates are

$$R_i = r_i(1 - \phi_A E_i(C_A))(1 - \phi_B E_i(C_B)), \quad (2)$$

$$D_i = \delta_i + (1 - \phi_A)E_i(C_A) + (1 - \phi_B)E_i(C_B), \quad (3)$$

$$G_i = R_i - D_i. \quad (4)$$

99 Our model is based on ‘Bliss independence’ (introduced in [38]) which assumes that the
 100 two drugs have distinct, independent, cellular targets and modes of action [39]. In the case of
 101 bactericidal drugs, the null model of no synergistic or antagonistic drug interaction is given by
 102 the total mortality rate from the drug combination equalling the sum of the mortality rates
 103 that would ensue with each drug used in isolation. However, for bacteriostatic drugs, a null
 104 interaction means that each drug reduces the replication rate by the same factor in combination
 105 as when used in isolation. For a cell to die, it is sufficient for *either* drug to cause its death
 106 (akin to a logical OR gate), so these terms are added, whereas for a cell to divide *both* pathways
 107 impacted by the drugs must remain functional (akin to a logical AND gate), so the terms are
 108 multiplied. [While other modeling choices were possible, this approach is reasonable as successful](#)
 109 [cell division requires each necessary pathway to be functioning, and thus the probabilities of](#)
 110 [each pathway being functional should be multiplied.](#)

111 We denote the probability of a cell division event leading to a j -resistant daughter cell as
 112 μ_j , and ignore back-mutations and the (initially negligible) chance of double-mutations. We
 113 initially assume that the mutation rate is independent of the drug concentration used, though
 114 this assumption is later relaxed. Thus, a deterministic version of our model can be represented
 115 as the following system of ordinary differential equations (ODEs):

$$\begin{aligned} \frac{dS}{dt} &= S(R_S(1 - \mu_A - \mu_B) - D_S), \\ \frac{dM_A}{dt} &= M_A(R_{M_A} - D_{M_A}) + SR_S\mu_A, \\ \frac{dM_B}{dt} &= M_B(R_{M_B} - D_{M_B}) + SR_S\mu_B. \end{aligned} \quad (5)$$

116 Along with the initial conditions, where only susceptible cells are present ($S(0) = S_0$,
 117 $M_A(0) = 0$, $M_B(0) = 0$), this fully defines the mathematical model. To more realistically model
 118 the uncertainty inherent in growth and mutation, we employed a stochastic version of this

119 model. Specifically, for the computational implementation, we used the Stochastic Simulation
 120 Algorithm (also known as the Gillespie algorithm [40]) to evolve the system over time, with
 121 birth and death events given in Table 2. All simulations were performed using R v4.3.0 [41]. To
 122 make evolving this stochastic system ~~less computationally intensive~~ computationally feasible, we
 123 used tau-leaping to perform many transitions in one step with the *adaptivetau* package [42, 43].
 124 We used the *future* package to parallelise simulation runs [44]. To store, analyse, and visualise
 125 the simulation data we used the *tidyverse* set of packages [45, 46].

Table 2: Transition events and rates for the Gillespie algorithm.

Event	Transition	Rate
S birth	$S \rightarrow S + 1$	$SR_S(1 - \mu_A - \mu_B)$
M_A birth	$M_A \rightarrow M_A + 1$	$SR_S\mu_A + M_AR_{M_A}$
M_B birth	$M_B \rightarrow M_B + 1$	$SR_S\mu_B + M_BR_{M_B}$
S death	$S \rightarrow S - 1$	SD_S
M_A death	$M_A \rightarrow M_A - 1$	$M_AD_{M_A}$
M_B death	$M_B \rightarrow M_B - 1$	$M_BD_{M_B}$

126 The value we seek to maximise is the probability that the susceptible population is driven to
 127 extinction without resistance becoming established. This can be operationalised as the probabilit-
 128 ity that $S(t) + M_A(t) + M_B(t) = 0$ for any time t . Trivially, arbitrarily large drug concentrations
 129 are optimal for this goal. However, toxic side effects for the host mean that drug concentrations
 130 must be restricted. We use a simple toxicity model with some fixed maximum allowable toxic-
 131 ity c , and both drugs contribute equally and linearly to this maximum, that is $C_A + C_B \leq c$.
 132 To maximise the combined efficacy of the drugs, the highest allowable concentrations are used
 133 ($C_A + C_B = c$).

134 The drugs are assumed to be equally effective, and their concentrations are scaled to be
 135 in units standardised to the potency of the drug in question, such that $z_{S,A} = z_{S,B} = 1$. We
 136 initially assume complete resistance ($z_{M_A,A}, z_{M_B,B} = \infty$) and a default of no cross-resistance or
 137 collateral sensitivity such that $z_{M_A,B} = z_{M_B,A} = 1$. We use a default value of the maximum
 138 replication rate of $r_i = 1 \text{ h}^{-1}$, and of the (dimensionless) Hill coefficient of $\beta = 1$, using
 139 convenient round numbers that are realistic for some bacteria and drugs [47]. Denoting the total
 140 chance of a mutation conferring resistance as $\mu = \mu_A + \mu_B$, we use $\mu = 10^{-9}$ per replication
 141 which is in the range of common values in Table 1. We use a starting population size of
 142 $S_0 = 10^9$ cells and an intrinsic death rate of $\delta = \frac{1}{3} \text{ h}^{-1}$, which ~~allows resistance to occur~~
 143 ~~sometimes but not inevitably, and which~~ are plausible biological values [48]. Common values of
 144 the maximum drug-induced death rate of bactericidal drugs are anywhere from approximately
 145 1 h^{-1} to 10 h^{-1} [47]. However, the theoretical maximum efficacy of a bacteriostatic drug is
 146 1, that is preventing 100% of replications. To avoid skewing the model towards bactericidal
 147 drugs, we use a default value of 1 for the maximum drug-induced death rate too, which is
 148 at the lower end of common values. We chose all these parameter values first and foremost
 149 to ensure resistance evolves a middling fraction of the time - resistance occurring almost never
 150 or always would not yield biologically interesting phenomena - while using roughly plausible
 151 round values, rather than focusing on precise estimates from the empirical literature.~~The more~~

152 ~~important point for this simple theoretical model is to use parameter values that highlight~~
153 ~~biologically relevant phenomena, rather than using maximally likely parameter values.~~

154 Holding all other parameters constant, we seek a mapping $(\mu_A, \mu_B) \rightarrow (C_A, C_B)$ that max-
155 imises the probability of eventual extinction, P_E . We call a *strategy* a choice of what drug
156 concentrations $C_A \in [0, c]$ and $C_B = c - C_A$ to apply. Drugs for which resistance mutations
157 arise at a lower rate are preferred, however the diminishing marginal returns to increasing drug
158 concentrations defined by the $E_i(C_j)$ function mean that it is not necessarily optimal to use
159 only the drug with a lower mutation rate.

160 3 Results

161 3.1 Analytical solution

162 To find the probability P_D that a newly arisen resistant mutant cell leaves no descendants in the
163 distant future, we can use the law of total probability, noting that a mutant is either resistant
164 to A or B . Denoting ~~the total probability of a mutation conferring resistance as $\mu = \mu_A + \mu_B$,~~
165 ~~and~~ the probability a strain- i mutant cell leaves no descendants in the distant future as $P_{D|i}$,
166 we get

$$P_D = \frac{\mu_A}{\mu} P_{D|M_A} + \frac{\mu_B}{\mu} P_{D|M_B}. \quad (6)$$

167 Due to the stochastic nature of the model, even a mutant lineage with a positive growth
168 rate may become extinct, and thus $P_{D|i}$ is not necessarily 0. We can again use the law of total
169 probability, noting that the cell must either die before dividing or divide before dying, and that
170 the probability of each occurring first is proportional to the rate of that stochastic process. If
171 the cell successfully divides once, each of the two daughter cells will also have a $P_{D|i}$ chance of
172 leaving no descendants, as they are functionally identical and independent. This gives

$$P_{D|i} = \frac{D_i}{R_i + D_i} \cdot 1 + \frac{R_i}{R_i + D_i} \cdot P_{D|i}^2. \quad (7)$$

173 This is a special case of the well-characterised Gambler's Ruin problem, where a bettor
174 repeatedly wagers to either gain or lose a single dollar, until either they have lost everything, or
175 reached some target value. In our case, extinction occurs if and only if every lineage initiated
176 by a single mutant cell eventually dies out, and the solution known since Fermat [49] is that

$$P_{D|i} = \min\left(\frac{D_i}{R_i}, 1\right). \quad (8)$$

177 Now we can approximate the number of cell divisions (\mathcal{N}) in the susceptible population
178 as a deterministic process, as it begins with a very large number of cells so the stochasticity
179 of individual cell divisions becomes negligible. Given that $\mu \ll 1$ (see e.g. Table 1), we can

180 ignore losses from mutation and thus use the approximation $\frac{dS}{dt} \approx S(R_S - D_S)$ and therefore
 181 $S(t) \approx S_0 e^{(R_S - D_S)t}$. Given that under antibiotic treatment $R_S < D_S$ and hence $G_S < 0$, this
 182 means the susceptible population undergoes exponential decay. We can then estimate the total
 183 number of replications \mathcal{N} as

$$\begin{aligned} \mathcal{N} &= \int_0^\infty S(t) R_S dt \\ &\approx \frac{S_0}{\frac{D_S}{R_S} - 1}. \end{aligned} \quad (9)$$

184 The probability that each cell starts a successful resistant lineage is the product of the
 185 probability of a resistance mutation (μ) and the probability that a resistant mutant leaves
 186 descendants ($1 - P_D$). Noting that the outcome of each new cell is independent, we find the
 187 overall extinction probability is

$$P_E = (1 - \mu(1 - P_D))^{\mathcal{N}}. \quad (10)$$

188 Because $\mu \ll 1$, we can again make the approximation

$$\begin{aligned} P_E &= \exp(\mathcal{N} \ln(1 - \mu(1 - P_D))) \\ &\approx \exp(-\mu \mathcal{N}(1 - P_D)). \end{aligned} \quad (11)$$

189 This finding is structurally very similar to the classic result from the evolutionary rescue
 190 theory literature that $P_E \approx \exp(-N_0 \theta)$ where N_0 is the initial population introduced to a
 191 novel environment, and θ is the rate of rescue for each individual [50]. In our case, \mathcal{N} replaces
 192 N_0 given the relevant quantity is the number of replications, not the inoculum size, and θ is
 193 replaced by the probability a mutation occurs and survives, $\mu(1 - P_D)$.

194 Equation 11 will be used for the computational implementation, as complicated expressions
 195 are unproblematic for numerical methods. But to make further analytical progress, it is useful to
 196 simplify the analysis by considering a small class of possible parameters that make the formulas
 197 collapse down to more manageable forms. In particular, the simplifying assumptions are:

- 198 • Resistant cells are unaffected by arbitrarily high drug concentrations ($E_{M_A}(C_A) = 0$,
 199 $E_{M_B}(C_B) = 0$ for all drug concentrations $C_A, C_B \in \mathbb{R}^+$).
- 200 • The shape parameters of the pharmacodynamic functions are unity ($\beta_A = \beta_B = 1$, equiv-
 201 alent to Michaelis-Menten kinetics).
- 202 • The drug-free replication rate and death rate of all strains are the same (that is, there is
 203 no cost of resistance: $r_i = r$, $\delta_i = \delta$).
- 204 • Both drugs are bacteriostatic ($\phi_A = \phi_B = 1$).
- 205 • When only drug A is applied ($C_A = c$, $C_B = 0$), the net growth rate of the susceptible and
 206 B -resistant strains are both zero ($G_S = G_{M_B} = 0$), and vice versa for when only drug B

207 is applied. (Even with both drugs being bacteriostatic, some replication events can occur,
 208 which is why the net growth rate is not negative.) This implies that $r = \delta(1 + c)$ and thus
 209 that $R_{M_A} = \delta \frac{1+c}{1+C_B} \geq \delta$ and likewise for M_B . Thus, $G_S \leq 0$ and $G_{M_A}, G_{M_B} \geq 0$. If the
 210 toxicity restriction were relaxed, and both drugs are used with a full dose ($C_A = C_B = c$)
 211 the population would be eradicated without resistance evolution as neither single-resistant
 212 strain could grow.

213 These simplifying assumptions may in reality often be violated, but they are [plausible](#)
 214 ~~simplifications~~[directionally plausible](#). For example, some resistance mutations do confer re-
 215 sistance even to relatively high drug concentrations [51], and costs of resistance can be small
 216 [52]. The final assumption is less conceptually important, but makes the computations simpler.
 217 While restrictive, these assumptions are still plausible enough to be interesting, and will be
 218 relaxed later in the [Simulations](#) section. After some algebraic manipulations, substituting these
 219 assumptions into equation 11 yields

$$\mathcal{N} = \frac{S_0(1+c)}{C_A C_B}, \quad (12)$$

$$1 - P_D = \frac{\mu_A C_A + \mu_B C_B}{\mu(1+c)}, \quad (13)$$

$$P_E = \exp\left(-S_0 \left(\frac{\mu_A}{C_B} + \frac{\mu_B}{C_A}\right)\right). \quad (14)$$

220 These are pleasingly interpretable equations. \mathcal{N} is minimised when $C_A = C_B$ given the
 221 diminishing marginal efficacy of each drug (Equation 12). Conversely, if only A or B is used
 222 [\(that is, \$C_B = 0\$ or \$C_A = 0\$, respectively\)](#), \mathcal{N} is unbounded, as the susceptible population is not
 223 killed. [The survival probability of a mutant is more sensitive to an increase in concentration](#)
 224 [of the drug to which resistance mutations arise more frequently](#)~~The probability of a resistant~~
 225 ~~mutant surviving increases when the drug to which resistance mutations arise more frequently~~
 226 ~~is used in a higher dose~~ (Equation 13). Finally, as μ_A increases relative to μ_B the infection is
 227 more likely to be cleared with a higher dose of drug B than drug A , because A -resistant cells
 228 are still susceptible to drug B (Equation 14).

229 We maximised P_E by computing its derivative with respect to C_A , setting this equal to 0,
 230 and solving for the optimal drug concentrations, denoted \hat{C}_A and \hat{C}_B , [to find that](#)

$$\hat{C}_A = \frac{c}{1 + \sqrt{\frac{\mu_A}{\mu_B}}}, \quad \hat{C}_B = \frac{c}{1 + \sqrt{\frac{\mu_B}{\mu_A}}}. \quad (15)$$

231 [This can also be rewritten in ratio form:](#)~~This yields the surprisingly simple solution that~~

$$\frac{\hat{C}_A}{\hat{C}_B} = \sqrt{\frac{\mu_B}{\mu_A}}, \quad \text{or} \quad (16)$$

$$\log\left(\frac{\hat{C}_A}{\hat{C}_B}\right) = -\frac{1}{2} \log\left(\frac{\mu_A}{\mu_B}\right).$$

232 The second version of this equation is useful as it shows that in log-log space there should be
 233 a linear relationship between the ratio of the mutation rates and the ratio of the doses. In other
 234 words, there is a power law relationship between the ratios of mutation rates and the ratio of
 235 optimal drug doses, with an exponent of $-\frac{1}{2}$. This relationship exhibits the expected behaviour
 236 whereby $\mu_A \rightarrow 0$ entails $\hat{C}_B \rightarrow 0$ and $\mu_B \rightarrow 0$ entails $\hat{C}_A \rightarrow 0$. This means, as mutations become
 237 more biased towards conferring resistance to one drug, the optimal combination dosing strategy
 238 relies more on the other, less resistance-prone, drug. However, even with a large difference in
 239 the mutation rates of the two drugs, the diminishing marginal efficacy of each drug defined by
 240 the $E_i(C_j)$ function means that a nonzero amount of the more resistance-evolution-prone drug
 241 should still be used in the drug cocktail.

242 In the case of both drugs being bactericidal, the intermediate steps are more complicated so
 243 are omitted here, but computations in Mathematica v13.1.0.0 [53] show that this same simple
 244 relationship in Equation 16 between mutation rates and optimal dosing ratios holds.

245 3.2 Simulations

246 Here, we corroborate the analytical findings computationally and explore regions of parameter
 247 space that appear inaccessible analytically.

248 When both drugs are bactericidal or both are bacteriostatic, the relationship given in Equa-
 249 tion 16 holds ([that is, the yellow computational and green theoretical lines coincide in Figure](#)
 250 [1A,D](#)). Interestingly, the actual values of P_E differ in the two cases, but the optimal dosing
 251 strategy remains the same. When both drugs are bacteriostatic, P_E is lower, as the susceptible
 252 population remains large for longer, given there is no drug-induced death (only the intrinsic
 253 death rate). A qualitatively similar relationship holds when one drug is bacteriostatic and
 254 the other is bactericidal, but the optimal dosing strategy is biased towards the bacteriostatic
 255 drug (Figure 1B,C). This effect, where the coupling of mutations to replications favours the
 256 growth-inhibiting activity of bacteriostatic drugs, was recently explored in [36].

257 Having verified the basic analytical findings, we can begin relaxing various assumptions.
 258 [We first relax the unrealistic assumption of complete resistance \(where \$E_{M_A}\(C_A\) = 0\$ and](#)
 259 [\$E_{M_B}\(C_B\) = 0\$ for all drug concentrations, implying \$z_{M_A,A} = z_{M_B,B} = \infty\$ \).](#) In reality, each
 260 [resistant strain is still affected by high drug concentrations to some varying extent. To model](#)
 261 [this, for each simulation run we pick resistance values from a shifted exponential distribution](#)
 262 [\$z_{M_A,A}, z_{M_B,B} \sim 1 + \text{Exp}\(\frac{1}{\zeta-1}\)\$ with mean \$\zeta > 1\$. The shift ensures that resistant strains are](#)
 263 [always more resistant than the susceptible strain \(\$z_{M_A,A} > z_{S,A} = 1\$ and \$z_{M_B,B} > z_{S,B} = 1\$ \). \(In](#)
 264 [reality, some mutations would increase drug susceptibility, but these are not modelled as they](#)
 265 [would be quickly eliminated from the population.\) The exponential shape of the distribution](#)
 266 [reflects that there are many potential mutations conferring weak resistance and fewer mutations](#)
 267 [conferring strong resistance \[51\]. Under this model, some mutants will have low \$z_{M_A,A}\$ or \$z_{M_B,B}\$](#)
 268 [values that entail negative growth rates for therapeutic drug concentrations, making them](#)
 269 [evolutionary dead ends. In other words, some mutants will sit outside of the mutant-selection](#)

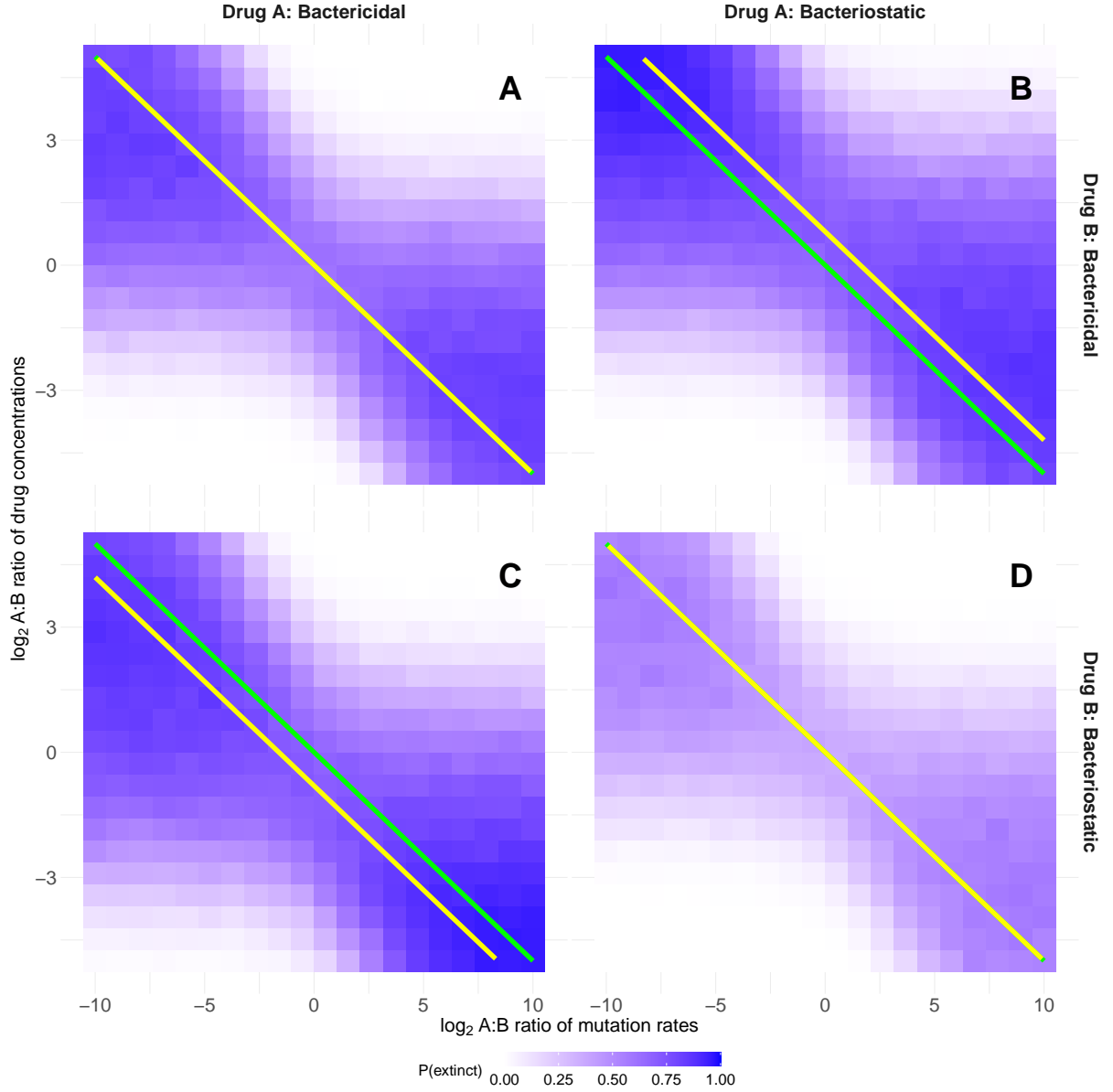


Figure 1: Computational corroboration of basic analytical results. Each grid square shows the probability that an initial population of susceptible bacteria will be driven to extinction by that dosing strategy, averaged over 1000 stochastic simulation runs. The yellow lines show the theoretically optimal dosing strategy for any given ratio of resistance mutation rates, determined by numerically evaluating P_E for many values of C_A and $C_B = c - C_A$ using Equation 11, and choosing the minimand and minimum. The green lines are the same in all panels and show the analytical result from Equation 16 for the basic scenario, for comparison. Parameter values are $\mu = 10^{-9}$, $S_0 = 10^9$, $r = 1$, $\delta = \frac{1}{3}$, $c = 2$, $\beta = 1$ and the drug modes of action vary in each panel. A) $\phi_A = \phi_B = 0$. B) $\phi_A = 1$, $\phi_B = 0$. C) $\phi_B = 1$, $\phi_A = 0$. D) $\phi_A = \phi_B = 1$.

270 window, which effectively reduces the mutation rate by eliminating some fraction of mutations
 271 [54]. As resistance becomes weaker (from the earlier unrealistic supposition of total resistance),
 272 the two resistant strains become less perfectly adapted to their respective drugs, and may even
 273 have negative growth rates. Further, in practice, bacteria may acquire different mutations
 274 conferring varying degrees of resistance. To incorporate this, we reran the simulations with
 275 each run having the EC_{50} values ($z_{i,j}$) of both mutant strains drawn independently from an
 276 exponential distribution with mean ζ . This is reflective of the fact that there are many potential
 277 mutations conferring weak resistance and fewer potential mutations conferring strong resistance
 278 available in the space of possible mutations [51]. This assumption of a distribution of mutational
 279 effects reduces the ‘effective’ mutation rate, as now some A and B -resistant mutants have low
 280 $z_{M_A,A}$ and $z_{M_B,B}$ values respectively (weak resistance). Such mutations will have a negative
 281 net growth rate, and hence are evolutionary dead ends.

282 For a fixed mutation rate ratio and two bacteriostatic drugs, as resistance becomes weaker
 283 ($\zeta \rightarrow 1$) the probability of extinction tends towards 1 and the optimal strategy tends towards
 284 using equal amounts of both drugs (Figure 2). This is because, given the diminishing marginal
 285 efficacy of increased doses of each drug, using equal concentrations minimises the net growth rate
 286 and therefore reduces \mathcal{N} , which is most important when the drugs are less effective. Conversely,
 287 for strong resistance as $\zeta \rightarrow \infty$, the optimal ratio of drug concentrations converges to the
 288 theoretical value given in Eq. 16 (which for the example in Figure 2 computes to $\log_2(\frac{\hat{C}_A}{\hat{C}_B}) =$
 289 $-\frac{1}{2} \log_2(\frac{1}{8}) = \frac{3}{2}$). Figure S1 shows that with $\zeta = 5$ the results are very similar to those seen
 290 in Figure 1. This suggests that our analytical results are still reasonable despite assuming
 291 resistance is complete.

292 Changing the shape parameter (β) noticeably changes the basic result. If $\beta > 1$ then the
 293 pharmacodynamic function has a sigmoidal shape and thus is steeper around the z -value where
 294 the drug has half its maximal effect. This means that intermediate values of both drugs are
 295 less beneficial than a more potent dose of just one drug, especially when both drugs are bac-
 296 teriostatic. Beyond some threshold β value, using just one drug is optimal (Figure 3). At
 297 this threshold value the intermediate drug concentration ratio switches from being the global
 298 maximum of extinction probability to only a local maximum, so an underlying smooth function
 299 leads to a discontinuous result upon taking the maximand. If instead $\beta < 1$ then the pharma-
 300 codynamic function is steep initially near a drug concentration of zero, and then approaches
 301 the maximum inhibitory effect slowly. Thus, it is most valuable to use some of both drugs.
 302 And again, below some threshold, using equal quantities of both drugs is optimal. Results for
 303 different mutation rate ratios and drug types are shown in Figures S2 and S3 for $\beta = 3$ and
 304 $\beta = 0.2$ respectively.

305 Thus far cost-free resistance has been assumed, whereas in reality mutations that confer
 306 resistance often reduce the maximum replication rate or cause other fitness costs. While some
 307 drugs give rise to resistant mutants with unchanged or even increased fitness in the absence
 308 of the drug, a meta-analysis suggests that common values of fitness costs are on the order of
 309 10% [52]. For the basic model, in the limit as $C_B \rightarrow 0$, δ was chosen such that $G_{M_B} \rightarrow 0$,

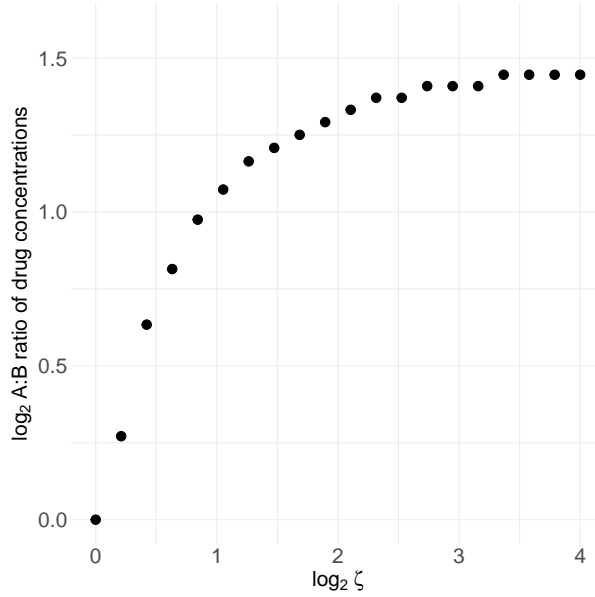


Figure 2: Optimal dosing with partial resistance. Parameters are the same as in Figure 1D except that $\mu_B = 8\mu_A$ and $z_{M_A,A}, z_{M_B,B} \sim 1 + \text{Exp}(\frac{1}{\zeta-1})$ for $\zeta > 1$ and $z_{M_A,A}, z_{M_B,B} = 1$ for $\zeta = 1$. For each dot defining a ζ value, 1000 values of z were drawn, evenly spaced from the cdf at the 0.1th, 0.2th, ..., 99.9th percentiles, and the mean probability of extinction was computed over these 1000 using the approximation in Equation 11. This was done for 30 possible ratios of drug doses, and the dosing ratio which yielded the highest P_E value was plotted on the y-axis.

310 whereas once resistance costs are introduced [by setting the replication rate of mutants to be](#)
311 [below that of the susceptible strain \(\$r_{M_A} = r_{M_B} = r_S \times \(1 - 0.1\) = 0.9\$ \)](#) the net growth rate of
312 mutants can become negative. There is a probability of 0 that a mutant with a negative growth
313 rate survives in the long term, and so all negative growth rates are equally good from the
314 perspective of minimising resistance evolution. Thus, here too intermediate dosing strategies
315 are sufficient to ensure $P_E \approx 1$ even for very skewed mutation rates (Figure S4). [Very skewed](#)
316 [drug concentrations also work equally well for very skewed mutation rates - because mutants](#)
317 [are less fit in this scenario, there is more flexibility in choosing a drug dosing ratio that results](#)
318 [in eradication.](#)

319 The toxicity-enforced limit of the total drug concentration has so far been fixed at $c = 2$,
320 but this limit is not biologically or theoretically special. We also considered a scenario where
321 the drugs are somewhat less toxic, and a larger maximum dose of $C_A + C_B \leq c = 5$ can be
322 applied. Maintaining the assumption from before that $G_S \leq 0$ and $G_{M_A}, G_{M_B} \geq 0$ we get that
323 $\delta = \frac{r}{1+c} = \frac{1}{6}$ is halved from its earlier value of $\delta = \frac{1}{3}$. This ensures we still explore an interesting
324 region of parameter space where mutants have a decent chance of arising and surviving. In this
325 case, we observe that the same basic trend holds, while the probability of extinction is higher
326 throughout (Figure S5). The higher overall drug concentrations mean that the optimal strategy
327 skews slightly more heavily towards the bacteriostatic drug (the yellow line is further away from
328 the green line in Figure S5 than in Figure 1) as in absolute terms this still leaves more of the
329 bactericidal drug to clear the infection.

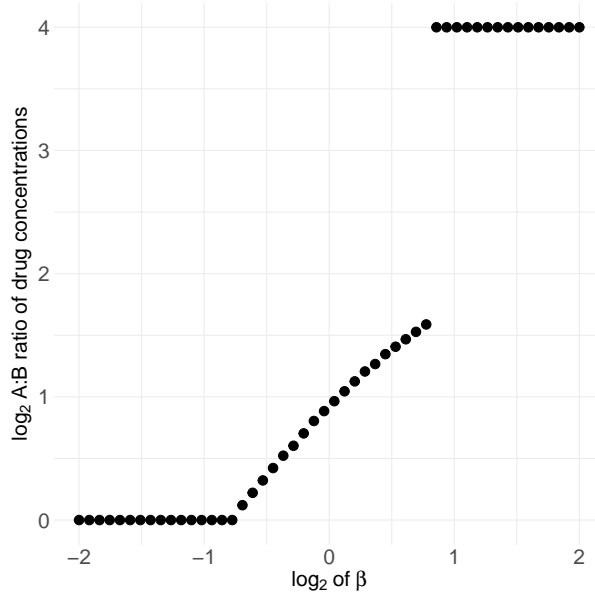


Figure 3: Optimal dosing under shape parameter variation. Parameters are the same as in Figure 1D except that the ratio of mutation rates is fixed at $\mu_B = 8\mu_A$ and $\delta = 1.1 - (1 + c^{-\beta})^{-1}$ which ensures that regardless of the value of β the susceptible population's growth rate is always at least slightly negative. The maximum drug concentrations ratio tried was $2^4 = 16$, so the fact that dots clump there does not suggest that value is special, instead that arbitrarily large ratios are optimal, but cannot readily be plotted on a finite y-axis.

330 We also extended our basic model to include pharmacokinetics, and found that introducing a
 331 drug decay rate of 0.15 h^{-1} left the basic results roughly unchanged (Figure S6). This suggests
 332 that ignoring pharmacokinetics in our analytical solution does not undermine its real-world
 333 applicability(as in the analytical solution) is not a fatal flaw.

334 Finally, we introduced resource constraints into our basic analytical model [36]. Each
 335 replication event uses one arbitrary unit of resource, and the simulation begins with 10^9 units
 336 of resource, with a constant influx of 10^8 h^{-1} . The maximum growth rate is now given by the
 337 Monod equation, with a resource affinity constant of 10^8 . Again, the basic relationship between
 338 mutation rate and optimal dosing concentrations persists (Figure S7). Now that growth is
 339 resource-limited, the susceptible population declines more rapidly, and there are fewer total
 340 replications \mathcal{N} , so across all panels and mutation rates the probability of extinction is higher. We
 341 model the resource-dependent bacterial growth using standard resource-consumption dynamics.
 342 Let $R(t)$ represent the concentration of the resource at time t in units standardised such that
 343 one cell division uses one unit of resource, and let the resource affinity constant be $K = 10^8$.
 344 The maximum growth rate of strain i without drugs is now given by the Monod equation
 345 [55] $r_i(R) = r_i \cdot \frac{R}{R+K}$ where r_i is the maximum growth rate in resource-unlimited conditions.
 346 This creates density-dependent growth that slows as resources become limiting. Let the initial
 347 resource level be $\rho = 10^9$ units, and the constant resource influx rate be $\omega = 10^8 \text{ h}^{-1}$. Then
 348 resource dynamics follow $\frac{dR}{dt} = \omega - (S \cdot R_S + M_A \cdot R_{M_A} + M_B \cdot R_{M_B})$ because each replication
 349 consumes one unit of resource. We selected parameter values that would allow for a meaningful
 350 comparison with our resource-unlimited model. The affinity constant $K = 10^8$ was chosen to

351 be an order of magnitude below the initial resource concentration ($\rho = 10^9$), ensuring that
352 growth begins near maximum rates but becomes resource-limited as the population expands.
353 The resource influx rate ($\omega = 10^8 \text{h}^{-1}$) was set to balance consumption when approximately 10^8
354 replications occur per hour.

355 As shown in Figure S7, the fundamental negative relationship between the optimal drug
356 concentration ratio ($\frac{\hat{C}_A}{\hat{C}_B}$) and mutation rate ratio ($\frac{\mu_A}{\mu_B}$) persists under resource-limited conditions,
357 consistent with our theoretical prediction. Though we do not show the theoretical yellow
358 curve for this scenario (as it was derived for resource-unlimited conditions), the computational
359 results still follow approximately the same slope in log-log space. With resource limitation, the
360 susceptible population reaches carrying capacity faster, reducing the total number of replications
361 \mathcal{N} before antibiotics take effect. This results in fewer mutation events and higher probabilities
362 of extinction across all scenarios compared to the resource-unlimited case. If we set resource
363 constraints to be very limiting, the choice of drugs would matter little, while conversely if
364 resource constraints were very light (e.g. $\rho = 10^{10}$) then the results diverge little from the
365 original resource-unconstrained model.

366 4 Discussion

367 Antimicrobial combination therapy is justified partly on the basis that it reduces the probabilit-
368 ity of infectious pathogens evolving resistance [1, 2]. To date, however, the design of optimal
369 dosing regimens in combination therapy has given little consideration to drug-specific variation
370 in pathogen resistance mutation rates. Here we have shown that as two drugs have increasingly
371 different mutation rates, the optimal dosing strategy entails using an increasingly large fraction
372 of the drug with a lower resistance mutation rate, according to a simple power law relation-
373 ship. This is an intuitive result, as drugs that have a higher resistance mutation rate are **riskier**
374 **less beneficial** to use. This result is relatively robust to changing the drugs' modes of action.
375 Across various alterations to the basic scenario — such as changes to the **pharmacodynamic**
376 shape parameter β , making resistance costly or incomplete, increasing the death rate, or adding
377 pharmacokinetics — the relationship between a skewed mutation rate and skewed optimal dos-
378 ing strategy persists, ~~but in several cases the dosing skew should never be raised above some~~
379 ~~maximum value.~~

380 Antibiotic resistance is particularly concerning in tuberculosis, where as of 2022, 12% of
381 all cases worldwide involved multidrug-resistant (MDR) strains of *M. tuberculosis* [56]. A key
382 component of an MDR containment strategy is to minimise the incidence of already resistant
383 strains acquiring resistance to another drug which was previously efficacious. Clinical data
384 from Georgia indicates that for MDR patients being treated with second-line antibiotics, 9%
385 acquire resistance to ofloxacin during treatment, and 10% to kanamycin [57]. To our knowledge,
386 there is no empirical data linking the probability of tuberculosis patients acquiring resistance
387 to a particular drug with the rate at which resistance mutations to that drug arise in the
388 laboratory, however there is a strong prima facie reason to expect such a connection. Mutation

389 rate differences among strains of *M. tuberculosis* have been investigated, and indeed a strain
 390 with more frequent mutations in the laboratory had elevated levels of MDR in clinical infections
 391 [58].

392 Our choices of functional forms for the drug-dependent mortality and replication rates in
 393 Equations 2 and 3 were crucial for the [analytical](#) results that followed. These are not the only
 394 reasonable choices, so bear some explanation and justification. Aside from our assumption of
 395 Bliss independence drug interaction, the other main model of null drug interactions is Loewe
 396 additivity (introduced in [59]). Loewe additivity assumes that the two drugs operate by the
 397 same mechanism of action, and therefore that the combined effect of both drugs is equivalent to
 398 the effect of either drug at their combined concentrations [19]. In this case, the mode of action
 399 and shape parameters of the two drugs must be equal, as by assumption the two drugs work
 400 interchangeably ($\beta_A = \beta_B = \beta, \phi_A = \phi_B = \phi$). Thus, under Loewe additivity we would have
 401 that

$$E_i(C_A, C_B) = \left(1 + \left(\frac{C_A}{z_{i,A}} + \frac{C_B}{z_{i,B}} \right)^{-\beta} \right)^{-1}, \quad (1')$$

$$R_i = r_i(1 - \phi E_i(C_A, C_B)), \quad (2')$$

$$D_i = \delta_i + (1 - \phi)E_i(C_A, C_B). \quad (3')$$

402 For the susceptible strain, recall that $z_{S,A} = z_{S,B} = 1$, and noting that $C_A + C_B = c$,
 403 we see that $E_S(C_A, C_B) = (1 + (C_A + C_B)^{-\beta})^{-1} = (1 + c^{-\beta})^{-1}$. That is, the effective drug
 404 concentration [for the susceptible strain](#) is only a function of the total drug concentration c ,
 405 but not dependent on the individual drug concentrations C_A and C_B . Therefore, the total
 406 number of replications \mathcal{N} will also be a function of c [only, regardless of how the total drug](#)
 407 [concentration is distributed between the two drugs. Unlike with Bliss independence where](#)
 408 [intermediate drug ratios provide more efficient killing due to diminishing returns of each drug,](#)
 409 [under Loewe additivity there is no efficacy difference when using more of one drug or the other.](#)
 410 ~~[As a result, unlike with Bliss independence, skewed drug dosing ratios do not clear the infection](#)~~
 411 ~~[slower.](#)~~ Thus, in the Loewe additivity model, there is no tradeoff between clearing an infection
 412 faster and more mutants arising, and it is always best to use only the drug that has a lower
 413 resistance mutation rate.

414 In our analysis and simulations, apart from the dosing concentration and resistance mutation
 415 rate, the two drugs had identical properties. This need not be the case. If drug A has a higher
 416 rate at which mutations conferring resistance to it arise, but it is also more potent per unit of
 417 toxicity, it may still be preferable to use a larger dose of it than drug B . Moreover, the toxicity
 418 model used here is unrealistic: in reality, there is no sharp cutoff [at \$c\$](#) beyond which further
 419 increases in drug doses [are not allowed because of](#) catastrophic consequences and before
 420 which toxicity is zero. Instead, negative side effects are likely to be a smooth monotonically
 421 increasing function of drug concentration [60], and it could be that the two drugs have additive,
 422 antagonistic, or synergistic combined effects on total toxicity. Allowing for this greater subtlety
 423 in drug toxicity would be a valuable avenue for further research, but could complicate the

424 mathematical analysis considerably.

425 One of the key weaknesses of the analytical solution presented here is that it relies on
426 constant replication and death rates over time for all strains, whereas in reality drugs decay
427 over time in the patient’s body. It appears that this simplification does not change the core
428 result, however, given the introduction of pharmacokinetics in Figure S6 left the main trend
429 unchanged. Our analytical results relied on assuming mutations confer complete resistance,
430 where for arbitrarily large drug concentrations the mutant still achieves a positive growth rate
431 (that is, the mutant selection window is infinitely wide). This is clearly unrealistic. Our
432 simulation results in Figures 2 and S1 show that relaxing this assumption to allow for a realistic
433 mutant selection window weakens but does not drastically change the result. The simulations
434 could be extended in many ways, such as including multiple species of commensal or pathogen
435 bacteria.

436 In our simulations, resource limitations led to reduced incidence of resistance mutants arising
437 and surviving. An important effect we did not include in our analytical model, and could not
438 detect in the simulations, is ‘competitive release’ where a strain or species that is initially limited
439 in its population size due to competition with a fit cohabitant, can begin to grow rapidly if the
440 competitor is eliminated [21, 61, 62]. In particular, if the susceptible bacterial population
441 reaches a high level, then resistant mutants may struggle to grow, but once antibiotics crash
442 the susceptible population, there is more ecological room for the resistant strains to grow. We
443 did not observe this effect, likely because there were no pre-existing mutants in our simulations,
444 and so even if the susceptible population crashes, there may be no resistant strain ready to fill
445 the newly vacated niche. Thus, exploring situations with some pre-existing mutants [18] could
446 be a valuable extension to our study.

447 Antimicrobial resistance is often conferred not by *de novo* mutations but through horizontal
448 gene transfer (HGT), e.g. through the transfer of plasmids (conjugation), or the uptake of free
449 DNA from the environment (transformation) [63, 64]. Whilst our model does not incorporate
450 HGT of resistance genes, we believe that in some situations our results may still be applicable,
451 at least approximately. For example, consider a scenario in which a drug-susceptible pathogen
452 co-occurs but is not in competition with resistant commensal bacteria, and that the resistance
453 genes can be transferred to the pathogen. In this situation, one would expect per capita rates of
454 HGT to be roughly constant over time. (Under the commonly used mass-action assumption, the
455 rate of HGT can be expressed as αSD , where S is the recipient and D the donor population size
456 [of resistant commensals, and \$\alpha\$ is a rate parameter.](#)) Therefore, within our model framework,
457 the process of HGT would be equivalent to the process of mutation (with αD corresponding to
458 the mutation rate μ), and our results would extend to mutations acquired through HGT or a
459 combination of both mutation and HGT. [It is important to caution though that the analogy
460 between mutation and HGT outlined above rests on the strong assumption that the number
461 of resistant donors remains constant through time.](#)~~Depending on the bacteria and mechanism
462 of HGT, rates of HGT are potentially orders of magnitude greater than mutation rates. Thus,
463 using a drug to which the commensal bacteria are susceptible could make resistance considerably~~

464 ~~less likely to evolve.~~ More complex scenarios where the donor populations are also affected by
465 the drug or interact with the pathogen population (e.g., through competition or cross-feeding)
466 would require a new model incorporating these effects.

467 While these results will take time to become clinically applicable, the potential of using
468 the (often well-characterised) resistance mutation rate in deciding on a treatment strategy is
469 unreasonably underexplored. Even if theoretical models as abstract and (compared to reality)
470 simple as this one cannot be directly applied in clinical settings, our results could motivate
471 experimental efforts to corroborate them, which could in turn lead to *in vivo* tests. Our findings
472 should in principle be straightforward to test in the laboratory. This would require assembling a
473 set of drugs with considerably different mutation rates in some model bacteria, and challenging
474 parallel susceptible populations with different pairs of these drugs in a variety of concentration
475 ratios. Integrating knowledge of resistance mutation rates into pharmacological decision-making
476 has the potential to clear more infections and minimise resistance evolution.

477 **Acknowledgements**

478 We would like to thank the Engelstädter and Letten groups for discussions on this topic, in
479 particular James Richardson and Christopher Brown. ChatGPT-4 and GitHub Copilot were
480 used for coding assistance (but did not write any part of the manuscript).

481 **Funding**

482 OD received a Vice-Chancellor’s Scholarship and Harriett Marks Bursary at the University
483 of Queensland. ADL is supported by Australian Research Council grants DP220103350 and
484 DE230100373. JE is supported by Australian Research Council grant DP190103039.

485 **Conflict of Interest Disclosure**

486 The authors declare they have no conflict of interest relating to the content of this article.

487 **Data and Code Availability**

488 All R and Mathematica code used to generate the figures and perform the symbolic manipula-
489 tions, respectively, is available at <https://zenodo.org/records/14197442>

490 **References**

- 491 1. Angst DC, Tepekule B, Sun L, Bogos B, and Bonhoeffer S. 2021 Comparing treatment
492 strategies to reduce antibiotic resistance in an in vitro epidemiological setting. *Proceedings*
493 *of the National Academy of Sciences of the United States of America*. 118 :e2023467118.
494 (doi:[10.1073/pnas.2023467118](https://doi.org/10.1073/pnas.2023467118))
- 495 2. Leekha S, Terrell CL, and Edson RS. 2011 *General Principles of Antimicrobial Therapy*.
496 *Mayo Clinic Proceedings*. 86 :156–67. (doi:[10.4065/mcp.2010.0639](https://doi.org/10.4065/mcp.2010.0639))
- 497 3. Nyhoegen C and Uecker H. 2023 Sequential antibiotic therapy in the laboratory and in
498 the patient. *J R Soc Interface*. 20 :20220793–20220793. (doi:[10.1098/rsif.2022.0793](https://doi.org/10.1098/rsif.2022.0793))
- 499 4. Imamovic L and Sommer MOA. 2013 Use of Collateral Sensitivity Networks to Design Drug
500 Cycling Protocols That Avoid Resistance Development. *Science Translational Medicine*. 5
501 :204ra132–204ra132. (doi:[10.1126/scitranslmed.3006609](https://doi.org/10.1126/scitranslmed.3006609))
- 502 5. Kim S, Lieberman TD, and Kishony R. 2014 Alternating antibiotic treatments constrain
503 evolutionary paths to multidrug resistance. *Proceedings of the National Academy of Sci-*
504 *ences*. 111 :14494–9. (doi:[10.1073/pnas.1409800111](https://doi.org/10.1073/pnas.1409800111))
- 505 6. Baym M, Stone LK, and Kishony R. 2016 Multidrug evolutionary strategies to reverse
506 antibiotic resistance. *Science*. 351 :aad3292. (doi:[10.1126/science.aad3292](https://doi.org/10.1126/science.aad3292))
- 507 7. Rao GG, Li J, Garonzik SM, Nation RL, and Forrest A. 2018 Assessment and modelling
508 of antibacterial combination regimens. *Clinical Microbiology and Infection*. 24 :689–96.
509 (doi:[10.1016/j.cmi.2017.12.004](https://doi.org/10.1016/j.cmi.2017.12.004))

- 510 8. Malik MA, Wani MY, and Hashmi AA. Chapter 1 - Combination therapy: Current status
511 and future perspectives. *Combination Therapy Against Multidrug Resistance*. Ed. by Wani
512 MY and Ahmad A. Academic Press, 2020 Jan 1:1–38. (doi:[10.1016/B978-0-12-820576-
513 1.00001-1](https://doi.org/10.1016/B978-0-12-820576-1.00001-1))
- 514 9. Siedentop B, Kachalov VN, Witzany C, Egger M, Kouyos RD, and Bonhoeffer S. 2024
515 The effect of combining antibiotics on resistance: A systematic review and meta-analysis.
516 medRxiv. :2023.07.10.23292374. (doi:[10.1101/2023.07.10.23292374](https://doi.org/10.1101/2023.07.10.23292374))
- 517 10. Spyridis NP, Spyridis PG, Gelesme A, Sypsa V, Valianatou M, Metsou F, Gourgiotis D,
518 and Tsolia MN. 2007 The effectiveness of a 9-month regimen of isoniazid alone versus
519 3- and 4-month regimens of isoniazid plus rifampin for treatment of latent tuberculosis
520 infection in children: results of an 11-year randomized study. *Clinical Infectious Diseases: An Official Publication of the Infectious Diseases Society of America*. 45 :715–22. (doi:[10.
521 1086/520983](https://doi.org/10.1086/520983))
- 523 11. Schmid A, Wolfensberger A, Nemeth J, Schreiber PW, Sax H, and Kuster SP. 2019
524 Monotherapy versus combination therapy for multidrug-resistant Gram-negative infec-
525 tions: Systematic Review and Meta-Analysis. *Scientific Reports*. 9 :15290. (doi:[10.1038/
526 s41598-019-51711-x](https://doi.org/10.1038/s41598-019-51711-x))
- 527 12. Temime L, Hejblum G, Setbon M, and Valleron AJ. 2008 The rising impact of mathemati-
528 cal modelling in epidemiology: antibiotic resistance research as a case study. *Epidemiology
529 & Infection*. 136 :289–98. (doi:[10.1017/S0950268807009442](https://doi.org/10.1017/S0950268807009442))
- 530 13. Birkegård AC, Halasa T, Toft N, Folkesson A, and Græsbøll K. 2018 Send more data:
531 a systematic review of mathematical models of antimicrobial resistance. *Antimicrobial
532 Resistance & Infection Control*. 7 :117. (doi:[10.1186/s13756-018-0406-1](https://doi.org/10.1186/s13756-018-0406-1))
- 533 14. Roemhild R, Gokhale CS, Dirksen P, Blake C, Rosenstiel P, Traulsen A, Andersson DI, and
534 Schulenburg H. 2018 Cellular hysteresis as a principle to maximize the efficacy of antibiotic
535 therapy. *Proceedings of the National Academy of Sciences*. 115 :9767–72. (doi:[10.1073/
536 pnas.1810004115](https://doi.org/10.1073/pnas.1810004115))
- 537 15. Udekwu KI and Weiss H. 2018 Pharmacodynamic considerations of collateral sensitivity
538 in design of antibiotic treatment regimen. *Drug Design, Development and Therapy*. 12
539 :2249–57. (doi:[10.2147/DDDT.S164316](https://doi.org/10.2147/DDDT.S164316))
- 540 16. Cisneros-Mayoral S, Graña-Miraglia L, Pérez-Morales D, Peña-Miller R, and Fuentes-
541 Hernández A. 2022 Evolutionary History and Strength of Selection Determine the Rate
542 of Antibiotic Resistance Adaptation. *Molecular Biology and Evolution*. 39 :msac185.
543 (doi:[10.1093/molbev/msac185](https://doi.org/10.1093/molbev/msac185))
- 544 17. Sutradhar I, Ching C, Desai D, Suprenant M, Briars E, Heins Z, Khalil AS, and Zaman
545 MH. 2021 Computational Model To Quantify the Growth of Antibiotic-Resistant Bacteria
546 in Wastewater. *mSystems*. 6 :e00360–21. (doi:[10.1128/mSystems.00360-21](https://doi.org/10.1128/mSystems.00360-21))

- 547 18. Hemez C, Clarelli F, Palmer AC, Bleis C, Abel S, Chindelevitch L, Cohen T, and Abel zur
548 Wiesch P. 2022 Mechanisms of antibiotic action shape the fitness landscapes of resistance
549 mutations. *Computational and Structural Biotechnology Journal*. 20 :4688–703. (doi:[10.1016/j.csbj.2022.08.030](https://doi.org/10.1016/j.csbj.2022.08.030))
550
- 551 19. Nyhoegen C, Bonhoeffer S, and Uecker H. 2024 The many dimensions of combination ther-
552 apy: How to combine antibiotics to limit resistance evolution. *Evolutionary Applications*.
553 17 :e13764. (doi:[10.1111/eva.13764](https://doi.org/10.1111/eva.13764))
- 554 20. Marrec L and Bitbol AF. 2020 Resist or perish: Fate of a microbial population subjected
555 to a periodic presence of antimicrobial. *PLOS Computational Biology*. 16 :e1007798.
556 (doi:[10.1371/journal.pcbi.1007798](https://doi.org/10.1371/journal.pcbi.1007798))
- 557 21. Czuppon P, Day T, Débarre F, and Blanquart F. 2023 A stochastic analysis of the interplay
558 between antibiotic dose, mode of action, and bacterial competition in the evolution of
559 antibiotic resistance. *PLOS Computational Biology*. 19 :e1011364. (doi:[10.1371/journal.pcbi.1011364](https://doi.org/10.1371/journal.pcbi.1011364))
560
- 561 22. Martinez JL and Baquero F. 2000 Mutation Frequencies and Antibiotic Resistance. *Anti-*
562 *microbial Agents and Chemotherapy*. 44 :1771–7. (doi:[10.1128/aac.44.7.1771-](https://doi.org/10.1128/aac.44.7.1771-1777.2000)
563 [1777.2000](https://doi.org/10.1128/aac.44.7.1771-1777.2000))
- 564 23. Chevereau G, Dravecká M, Batur T, Guvenek A, Ayhan DH, Toprak E, and Bollenbach T.
565 2015 Quantifying the Determinants of Evolutionary Dynamics Leading to Drug Resistance.
566 *PLOS Biology*. 13 :e1002299. (doi:[10.1371/journal.pbio.1002299](https://doi.org/10.1371/journal.pbio.1002299))
- 567 24. World Health Organisation. Tuberculosis (TB). 2023 Nov 7. Available from: <https://www.who.int/news-room/fact-sheets/detail/tuberculosis>
568
- 569 25. David HL. 1970 Probability Distribution of Drug-Resistant Mutants in Unselected Popu-
570 lations of *Mycobacterium tuberculosis*. *Applied Microbiology*. 20 :810–4. (doi:[10.1128/](https://doi.org/10.1128/am.20.5.810-814.1970)
571 [am.20.5.810-814.1970](https://doi.org/10.1128/am.20.5.810-814.1970))
- 572 26. Frenoy A and Bonhoeffer S. 2018 Death and population dynamics affect mutation rate
573 estimates and evolvability under stress in bacteria. *PLOS Biology*. 16 :e2005056. (doi:[10.1371/journal.pbio.2005056](https://doi.org/10.1371/journal.pbio.2005056))
574
- 575 27. Bergval IL, Schuitema ARJ, Klatser PR, and Anthony RM. 2009 Resistant mutants of
576 *Mycobacterium tuberculosis* selected in vitro do not reflect the in vivo mechanism of
577 isoniazid resistance. *Journal of Antimicrobial Chemotherapy*. 64 :515–23. (doi:[10.1093/](https://doi.org/10.1093/jac/dkp237)
578 [jac/dkp237](https://doi.org/10.1093/jac/dkp237))
- 579 28. Werngren J and Hoffner SE. 2003 Drug-Susceptible *Mycobacterium tuberculosis* Beijing
580 Genotype Does Not Develop Mutation-Conferred Resistance to Rifampin at an Elevated
581 Rate. *Journal of Clinical Microbiology*. 41 :1520–4. (doi:[10.1128/jcm.41.4.1520-](https://doi.org/10.1128/jcm.41.4.1520-1524.2003)
582 [1524.2003](https://doi.org/10.1128/jcm.41.4.1520-1524.2003))
- 583 29. Nyinoh IW. 2019 Spontaneous mutations conferring antibiotic resistance to antitubercu-
584 lar drugs at a range of concentrations in *Mycobacterium smegmatis*. *Drug Development*
585 *Research*. 80 :147–54. (doi:[10.1002/ddr.21497](https://doi.org/10.1002/ddr.21497))

- 586 30. Krašovec R, Belavkin RV, Aston JAD, Channon A, Aston E, Rash BM, Kadirvel M,
587 Forbes S, and Knight CG. 2014 Mutation rate plasticity in rifampicin resistance depends
588 on *Escherichia coli* cell–cell interactions. *Nature Communications*. 5 :3742. (doi:[10.1038/
589 ncomms4742](https://doi.org/10.1038/ncomms4742))
- 590 31. Spagnolo F, Rinaldi C, Sajorda DR, and Dykhuizen DE. 2016 Evolution of Resistance to
591 Continuously Increasing Streptomycin Concentrations in Populations of *Escherichia coli*.
592 *Antimicrobial Agents and Chemotherapy*. 60 :1336–42. (doi:[10.1128/aac.01359-15](https://doi.org/10.1128/aac.01359-15))
- 593 32. Huseby DL, Pietsch F, Brandis G, Garoff L, Tegehall A, and Hughes D. 2017 Mutation
594 Supply and Relative Fitness Shape the Genotypes of Ciprofloxacin-Resistant *Escherichia*
595 *coli*. *Molecular Biology and Evolution*. 34 :1029–39. (doi:[10.1093/molbev/msx052](https://doi.org/10.1093/molbev/msx052))
- 596 33. Meibohm B and Derendorf H. 1997 Basic concepts of pharmacokinetic/pharmacodynamic
597 (PK/PD) modelling. *International Journal of Clinical Pharmacology and Therapeutics*. 35
598 :401–13
- 599 34. Regoes RR, Wiuff C, Zappala RM, Garner KN, Baquero F, and Levin BR. 2004 Pharma-
600 codynamic Functions: a Multiparameter Approach to the Design of Antibiotic Treatment
601 Regimens. *Antimicrobial Agents and Chemotherapy*. 48 :3670–6. (doi:[10.1128/AAC.48.
602 10.3670-3676.2004](https://doi.org/10.1128/AAC.48.10.3670-3676.2004))
- 603 35. Neubig RR, Spedding M, Kenakin T, and Christopoulos A. 2003 International Union of
604 Pharmacology Committee on Receptor Nomenclature and Drug Classification. XXXVIII.
605 Update on Terms and Symbols in Quantitative Pharmacology. *Pharmacological Reviews*.
606 55 :597–606. (doi:[10.1124/pr.55.4.4](https://doi.org/10.1124/pr.55.4.4))
- 607 36. Delaney O, Letten AD, and Engelstädter J. 2023 Drug mode of action and resource con-
608 straints modulate antimicrobial resistance evolution. *bioRxiv*. (doi:[10.1101/2023.08.29.
609 555413](https://doi.org/10.1101/2023.08.29.555413))
- 610 37. Greischar MA, Alexander HK, Bashey F, Bento AI, Bhattacharya A, Bushman M, Childs
611 LM, Daversa DR, Day T, Faust CL, Gallagher ME, Gandon S, Glidden CK, Halliday
612 FW, Hanley KA, Kamiya T, Read AF, Schwabl P, Sweeny AR, Tate AT, Thompson RN,
613 Wale N, Wearing HJ, Yeh PJ, and Mideo N. 2020 Evolutionary consequences of feedbacks
614 between within-host competition and disease control. *Evolution, Medicine, and Public*
615 *Health*. 2020 :30–4. (doi:[10.1093/emph/eoaa004](https://doi.org/10.1093/emph/eoaa004))
- 616 38. Bliss CI. 1939 The Toxicity of Poisons Applied Jointly. *Annals of Applied Biology*. 26
617 :585–615. (doi:[10.1111/j.1744-7348.1939.tb06990.x](https://doi.org/10.1111/j.1744-7348.1939.tb06990.x))
- 618 39. Baeder DY, Yu G, Hozé N, Rolff J, and Regoes RR. 2016 Antimicrobial combinations: Bliss
619 independence and Loewe additivity derived from mechanistic multi-hit models. *Philosophical*
620 *Transactions of the Royal Society B: Biological Sciences*. 371 :20150294. (doi:[10.
621 1098/rstb.2015.0294](https://doi.org/10.1098/rstb.2015.0294))
- 622 40. Gillespie DT. 1976 A general method for numerically simulating the stochastic time evolu-
623 tion of coupled chemical reactions. *Journal of Computational Physics*. 22 :403–34. (doi:[10.
624 1016/0021-9991\(76\)90041-3](https://doi.org/10.1016/0021-9991(76)90041-3))

- 625 41. R Core Team. R: A Language and Environment for Statistical Computing. Version 4.3.0.
626 2023. Available from: <https://www.R-project.org/>
- 627 42. Cao Y, Gillespie DT, and Petzold LR. 2007 Adaptive explicit-implicit tau-leaping method
628 with automatic tau selection. *The Journal of Chemical Physics*. 126 :224101. (doi:[10.
629 1063/1.2745299](https://doi.org/10.1063/1.2745299))
- 630 43. Johnson P. adaptivetau: Tau-Leaping Stochastic Simulation. Version R package version
631 2.2-3. 2019. Available from: <https://CRAN.R-project.org/package=adaptivetau>
- 632 44. Bengtsson H. 2021 A Unifying Framework for Parallel and Distributed Processing in R
633 using Futures. *The R Journal* 13 :208–27. (doi:[10.32614/RJ-2021-048](https://doi.org/10.32614/RJ-2021-048))
- 634 45. Wickham H, Averick M, Bryan J, Chang W, McGowan LD, François R, Golemund G,
635 Hayes A, Henry L, Hester J, Kuhn M, Pedersen TL, Miller E, Bache SM, Müller K, Ooms
636 J, Robinson D, Seidel DP, Spinu V, Takahashi K, Vaughan D, Wilke C, Woo K, and
637 Yutani H. 2019 Welcome to the tidyverse. *Journal of Open Source Software* 4 :1686.
638 (doi:[10.21105/joss.01686](https://doi.org/10.21105/joss.01686))
- 639 46. Campitelli E. Multiple Fill and Colour Scales in 'ggplot2'. 2023. (doi:[10.5281/zenodo.
640 2543762](https://doi.org/10.5281/zenodo.2543762))
- 641 47. Czock D and Keller F. 2007 Mechanism-based pharmacokinetic-pharmacodynamic mod-
642 eling of antimicrobial drug effects. *Journal of Pharmacokinetics and Pharmacodynamics*.
643 34 :727–51. (doi:[10.1007/s10928-007-9069-x](https://doi.org/10.1007/s10928-007-9069-x))
- 644 48. Nielsen EI, Viberg A, Löwdin E, Cars O, Karlsson MO, and Sandström M. 2006 Semimech-
645 anistic Pharmacokinetic/Pharmacodynamic Model for Assessment of Activity of Antibac-
646 terial Agents from Time-Kill Curve Experiments. *Antimicrobial Agents and Chemother-*
647 *apy*. 51 :128. (doi:[10.1128/AAC.00604-06](https://doi.org/10.1128/AAC.00604-06))
- 648 49. Feller W. An introduction to probability theory and its applications. 3d ed. Wiley series
649 in probability and mathematical statistics. New York: Wiley, 1968
- 650 50. Martin G, Aguilée R, Ramsayer J, Kaltz O, and Ronce O. 2013 The probability of evo-
651 lutionary rescue: towards a quantitative comparison between theory and evolution ex-
652 periments. *Philosophical Transactions of the Royal Society B: Biological Sciences*. 368
653 :20120088. (doi:[10.1098/rstb.2012.0088](https://doi.org/10.1098/rstb.2012.0088))
- 654 51. Iglér C, Rolff J, and Regoes R. 2021 Multi-step vs. single-step resistance evolution under
655 different drugs, pharmacokinetics, and treatment regimens. *eLife*. 10 :e64116. (doi:[10.
656 7554/eLife.64116](https://doi.org/10.7554/eLife.64116))
- 657 52. Melnyk AH, Wong A, and Kassen R. 2014 The fitness costs of antibiotic resistance muta-
658 tions. *Evolutionary Applications*. 8 :273. (doi:[10.1111/eva.12196](https://doi.org/10.1111/eva.12196))
- 659 53. Wolfram Research Inc. Mathematica Version 13.1.0.0. 2022. Available from: [https://
660 www.wolfram.com/mathematica](https://www.wolfram.com/mathematica)
- 661 54. Drlica K. 2003 The mutant selection window and antimicrobial resistance. *Journal of*
662 *Antimicrobial Chemotherapy*. 52 :11–7. (doi:[10.1093/jac/dkg269](https://doi.org/10.1093/jac/dkg269))

- 663 55. Monod J. 1949 The Growth of Bacterial Cultures. *Annual Review of Microbiology*. 3 :371–
664 94. (doi:[10.1146/annurev.mi.03.100149.002103](https://doi.org/10.1146/annurev.mi.03.100149.002103))
- 665 56. Salari N, Kanjoori AH, Hosseinian-Far A, Hasheminezhad R, Mansouri K, and Moham-
666 madi M. 2023 Global prevalence of drug-resistant tuberculosis: a systematic review and
667 meta-analysis. *Infectious Diseases of Poverty*. 12 :57. (doi:[10.1186/s40249-023-01107-x](https://doi.org/10.1186/s40249-023-01107-x))
- 668 57. Kempker RR, Kipiani M, Mirtskhulava V, Tukvadze N, Magee MJ, and Blumberg HM.
669 2015 Acquired Drug Resistance in Mycobacterium tuberculosis and Poor Outcomes among
670 Patients with Multidrug-Resistant Tuberculosis. *Emerging Infectious Diseases*. 21 :992–
671 1001. (doi:[10.3201/eid2106.141873](https://doi.org/10.3201/eid2106.141873))
- 672 58. Ford CB, Shah RR, Maeda MK, Gagneux S, Murray MB, Cohen T, Johnston JC, Gardy
673 J, Lipsitch M, and Fortune SM. 2013 Mycobacterium tuberculosis mutation rate estimates
674 from different lineages predict substantial differences in the emergence of drug resistant
675 tuberculosis. *Nature genetics*. 45 :784–90. (doi:[10.1038/ng.2656](https://doi.org/10.1038/ng.2656))
- 676 59. Loewe S and Muischnek H. 1926 Über Kombinationswirkungen. *Naunyn-Schmiedebergs*
677 *Archiv für experimentelle Pathologie und Pharmakologie*. 114 :313–26. (doi:[10.1007/
678 BF01952257](https://doi.org/10.1007/BF01952257))
- 679 60. Lazarou J, Pomeranz BH, and Corey PN. 1998 Incidence of Adverse Drug Reactions
680 in Hospitalized Patients A Meta-analysis of Prospective Studies. *JAMA*. 279 :1200–5.
681 (doi:[10.1001/jama.279.15.1200](https://doi.org/10.1001/jama.279.15.1200))
- 682 61. Day T, Huijben S, and Read AF. 2015 Is selection relevant in the evolutionary emergence of
683 drug resistance? *Trends in Microbiology*. 23 :126–33. (doi:[10.1016/j.tim.2015.01.005](https://doi.org/10.1016/j.tim.2015.01.005))
- 684 62. Wale N, Sim DG, Jones MJ, Salathe R, Day T, and Read AF. 2017 Resource limitation pre-
685 vents the emergence of drug resistance by intensifying within-host competition. *Proceed-*
686 *ings of the National Academy of Sciences*. 114 :13774–9. (doi:[10.1073/pnas.1715874115](https://doi.org/10.1073/pnas.1715874115))
- 687 63. Durão P, Balbontín R, and Gordo I. 2018 Evolutionary Mechanisms Shaping the Mainte-
688 nance of Antibiotic Resistance. *Trends in Microbiology*. 26 :677–91. (doi:[10.1016/j.tim.
689 2018.01.005](https://doi.org/10.1016/j.tim.2018.01.005))
- 690 64. McInnes RS, McCallum GE, Lamberte LE, and Schaik W van. 2020 Horizontal transfer of
691 antibiotic resistance genes in the human gut microbiome. *Current Opinion in Microbiology*.
692 *Host-Microbe Interactions: Bacteria* 53 :35–43. (doi:[10.1016/j.mib.2020.02.002](https://doi.org/10.1016/j.mib.2020.02.002))

693 **Supplementary Figures**

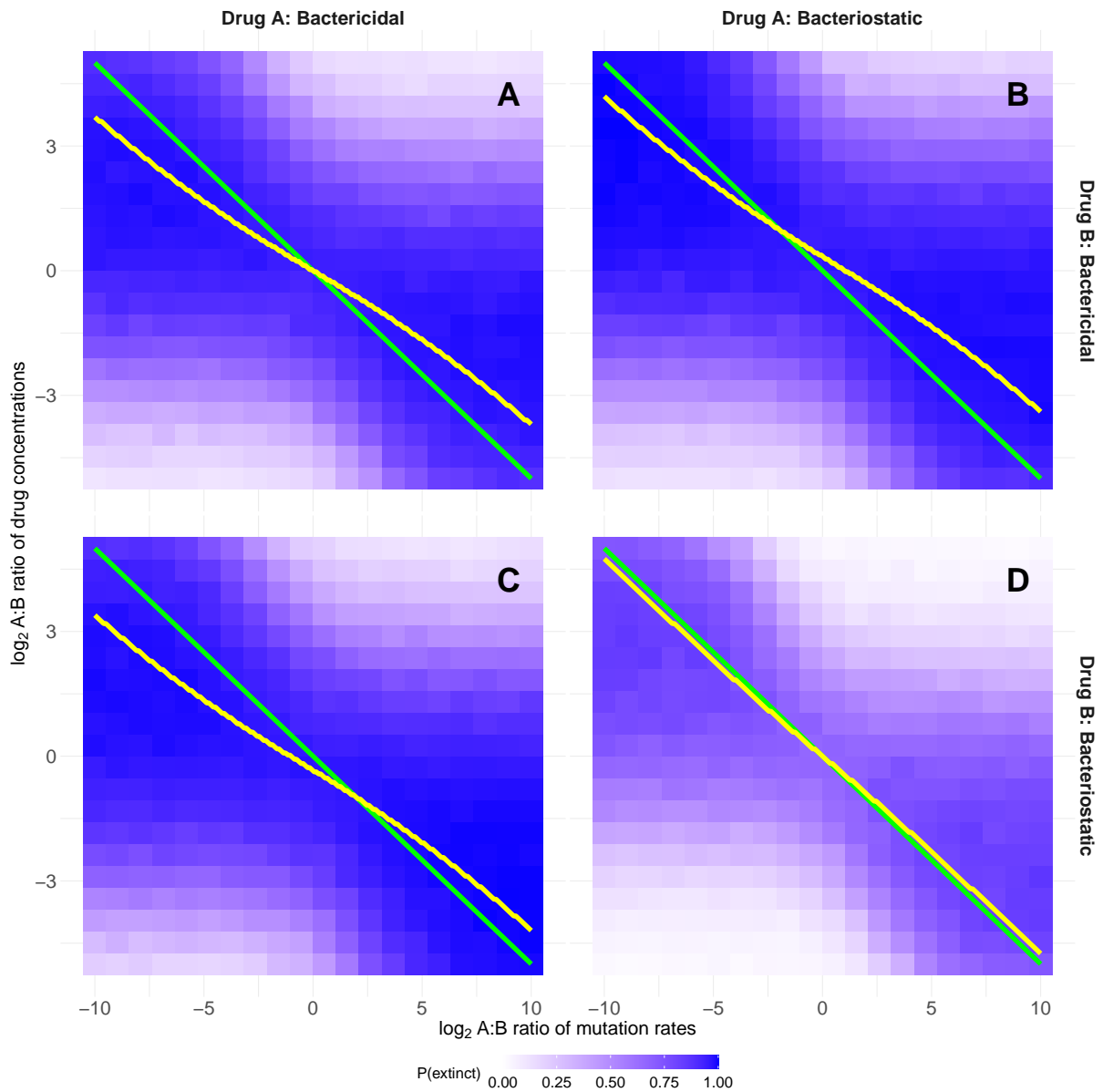


Figure S1: Optimal dosing with mutations conferring incomplete resistance. The parameters are identical to Figure 1 except $z_{M_{A,A}}, z_{M_{B,B}}, z_{M_{A,B}}, z_{M_{B,A}} \sim 1 + \text{Exp}(0.25)$, sampled independently for each run of the simulation.

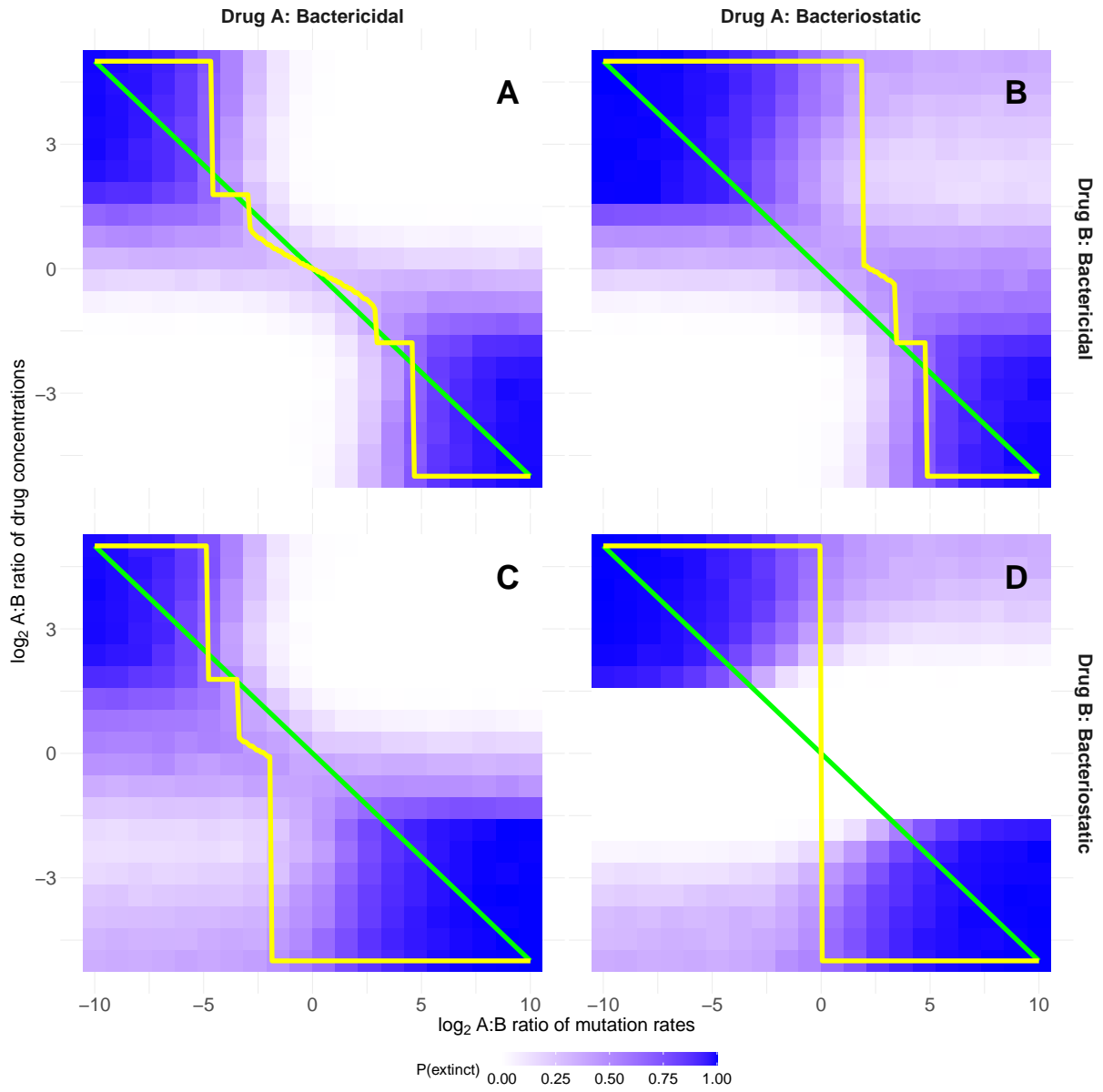


Figure S2: Optimal dosing with a larger shape parameter sometimes entails using solely one drug. The parameters are identical to Figure 1 except $\beta_A = \beta_B = 3$ and $\delta = 0.19$.

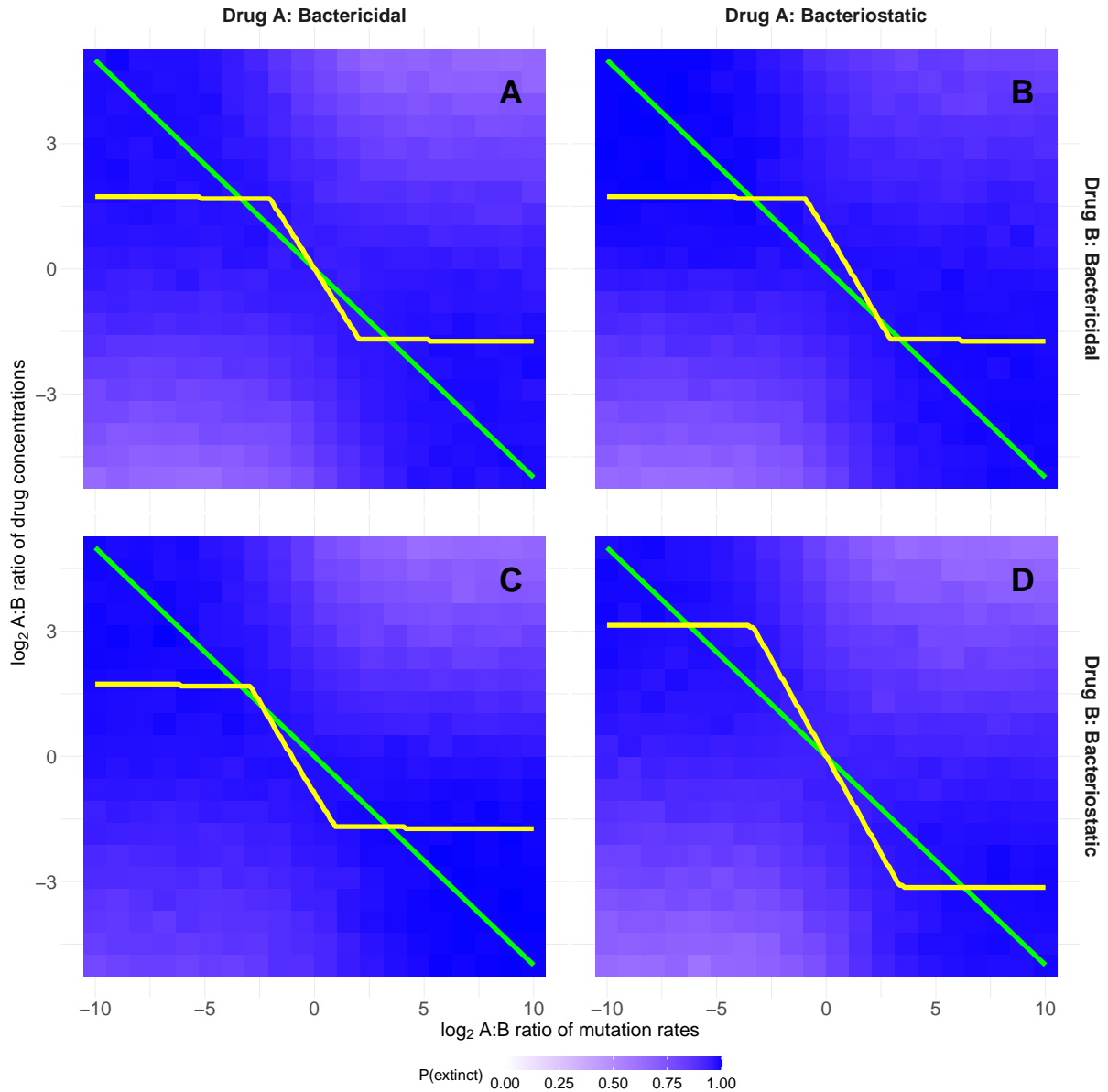


Figure S3: Optimal dosing with a smaller shape parameter ~~always includes non-zero amounts of both drugs~~. The parameters are identical to Figure 1 except $\beta_A = \beta_B = 0.2, \delta = 0.47$. In the top-left and bottom-right corners of each panel, $P_E = 1$ and so the precise drug concentration ratio used does not matter, as long as it is beyond some threshold. This is reflected in the z-shaped truncated yellow lines that do not require arbitrarily skewed drug dosing ratios.

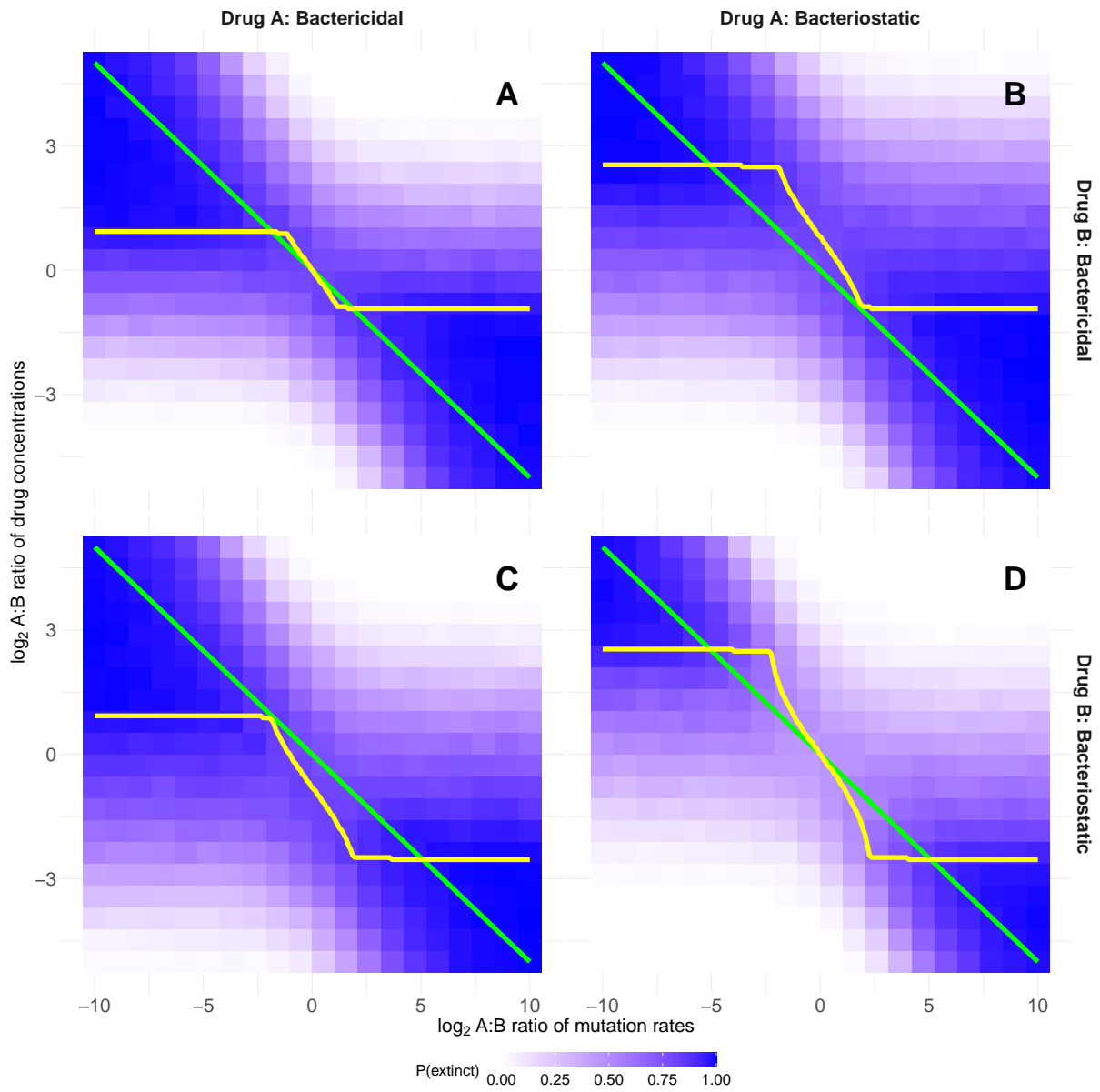


Figure S4: Optimal dosing with costs of resistance ~~always includes non-zero amounts of both drugs~~. The parameters are identical to Figure 1 except $r_{MA} = r_{MB} = r_S - 0.1 = 0.9$.

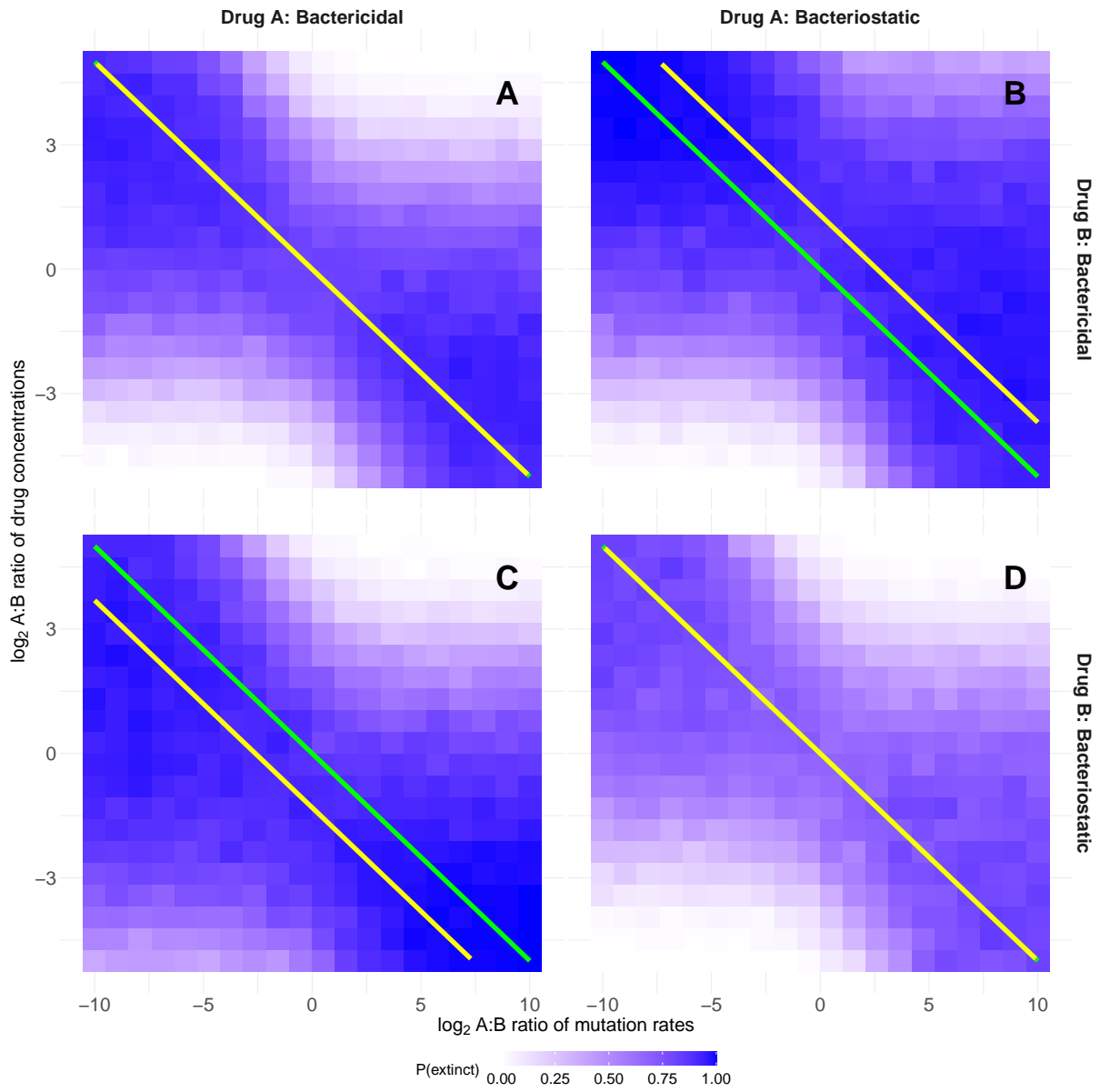


Figure S5: Optimal dosing with higher drug concentrations. The parameters are identical to Figure 1 except $c = 5, \delta = \frac{1}{6}$.

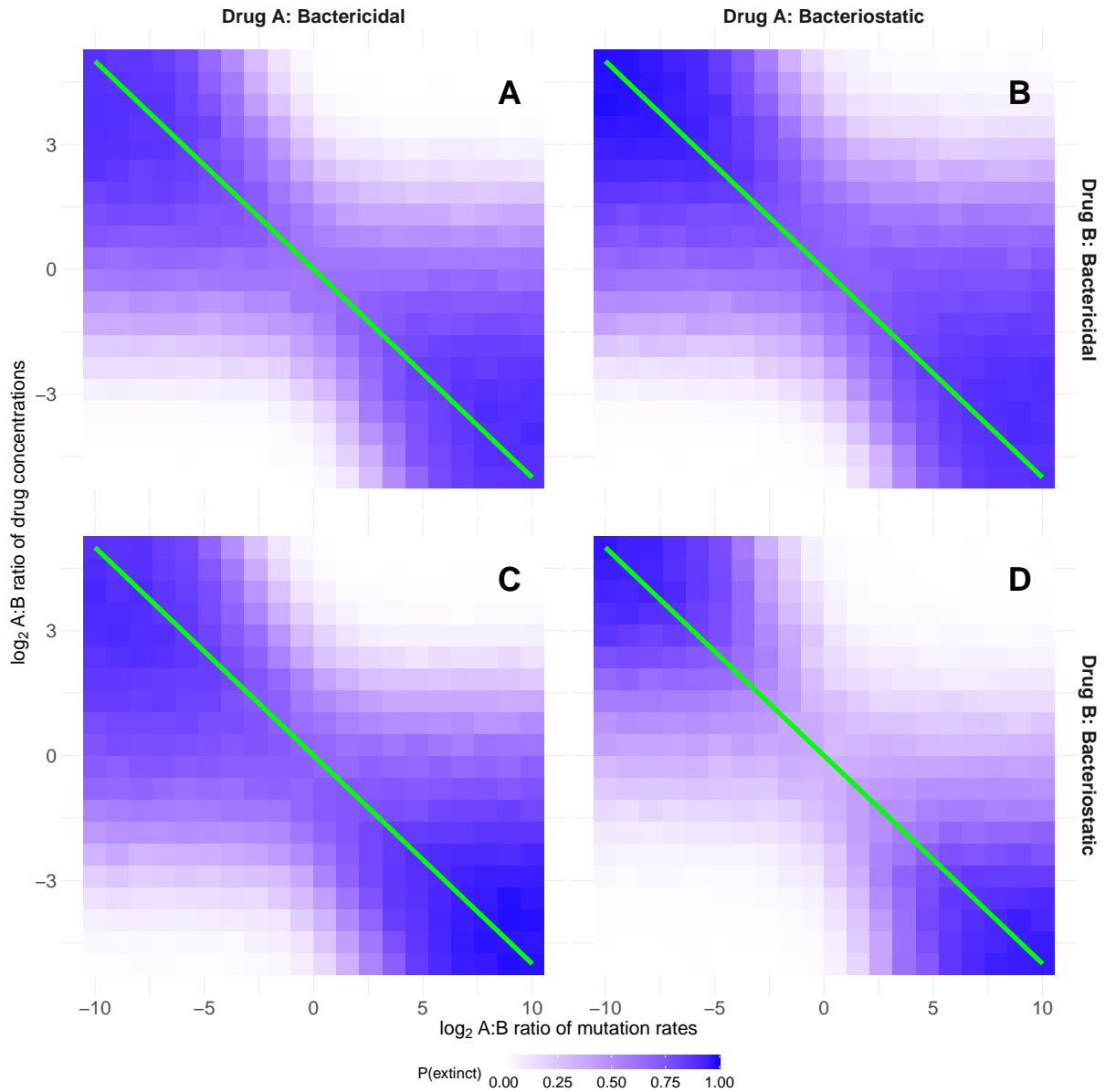


Figure S6: Optimal dosing with pharmacokinetics. The parameters are identical to Figure 1 except a drug decay rate of 0.15 has been introduced with doses every 12 hours of both drugs, meaning that $e^{-0.15 \times 12} = 17\%$ of the previous dose remains at the next dose. To compensate for the drug decaying, the intrinsic death rate has been increased by 0.2 to $\delta = 0.53$. The yellow theory lines are not shown here, as the theoretical analysis only dealt with constant drug concentrations. The original green lines are still shown for comparison.

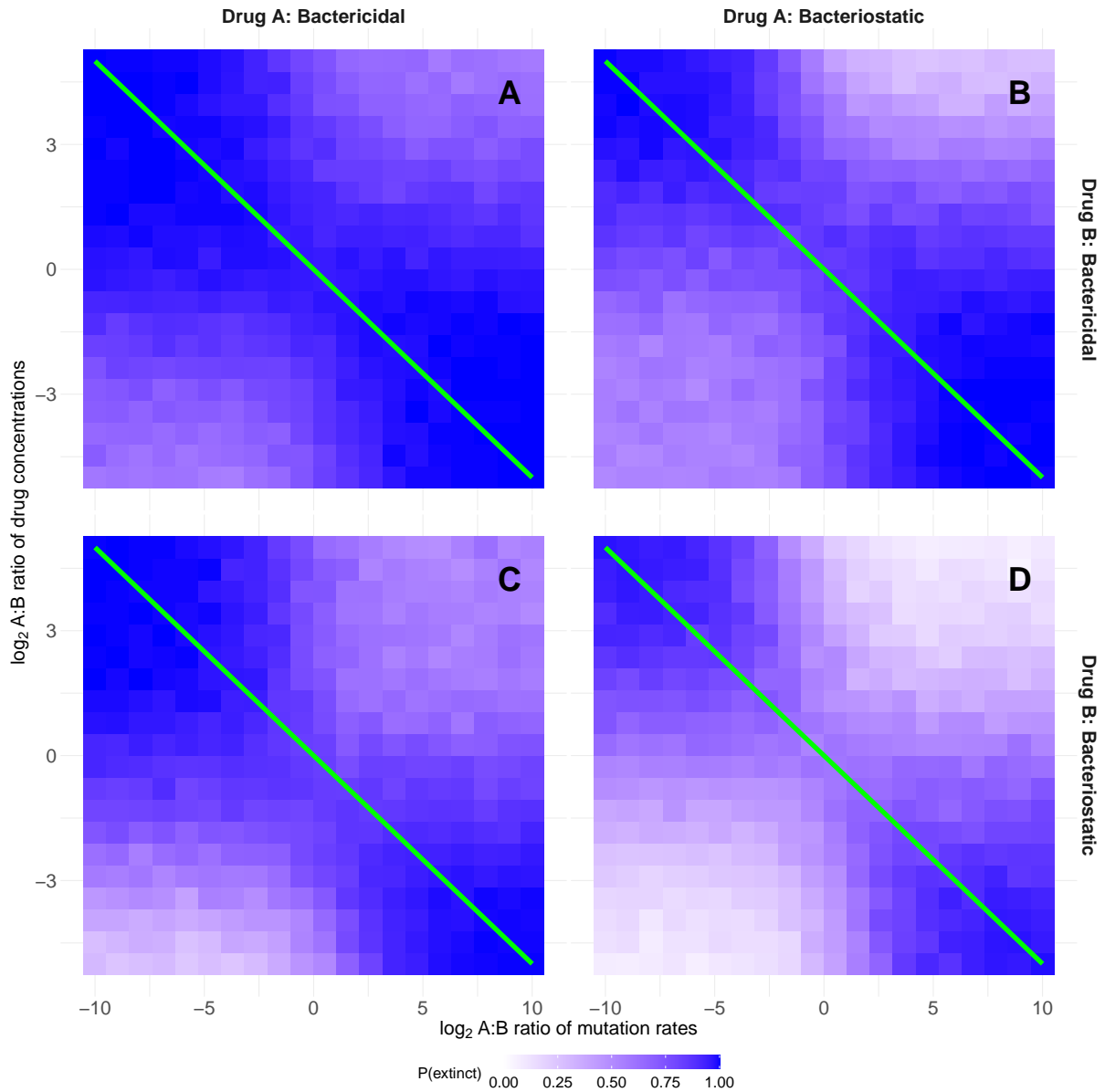


Figure S7: Optimal dosing with resource constraints. The parameters are identical to Figure 1 except growth is now modelled as being limited by a single rate-limiting resource, with an initial concentration of 10^9 units, where one unit is consumed per bacterial replication, and a constant [resource](#) influx of 10^8 h^{-1} . The yellow theory lines are not shown here, as the theoretical analysis [assumed unconstrained growth](#) ~~only dealt with constant drug concentrations~~. The original green lines are still shown for comparison.